Eur. Phys. J. C (2019) 79:280
https://doi.org/10.1140/epjc/s10052-019-6730-7

THE EUROPEAN PHYSICAL JOURNAL C

Regular Article - Experimental Physics

Search for dark matter produced in association with a Higgs boson decaying to a pair of bottom quarks in proton–proton collisions at $\sqrt{s} = 13\,\text{TeV}$

CMS Collaboration*

CERN, 1211 Geneva 23, Switzerland

Received: 15 November 2018 / Accepted: 26 February 2019

Abstract A search for dark matter produced in association with a Higgs boson decaying to a pair of bottom quarks is performed in proton–proton collisions at a center-of-mass energy of 13 TeV collected with the CMS detector at the LHC. The analyzed data sample corresponds to an integrated luminosity of $35.9\,\text{fb}^{-1}$. The signal is characterized by a large missing transverse momentum recoiling against a bottom quark–antiquark system that has a large Lorentz boost. The number of events observed in the data is consistent with the standard model background prediction. Results are interpreted in terms of limits both on parameters of the type-2 two-Higgs doublet model extended by an additional light pseudoscalar boson a (2HDM+a) and on parameters of a baryonic Z′ simplified model. The 2HDM+a model is tested experimentally for the first time. For the baryonic Z′ model, the presented results constitute the most stringent constraints to date.

1 Introduction

Astrophysical evidence for dark matter (DM) is one of the most compelling motivations for physics beyond the standard model (SM) [1–3]. Cosmological observations demonstrate that around 85% of the matter in the universe is comprised of DM [4] and they are largely consistent with the hypothesis that DM is composed primarily of weakly interacting massive particles. If nongravitational interactions exist between DM and SM particles, DM could be produced by colliding SM particles at high energy. Assuming the pair production of DM particles in hadron collisions occurs through a spin-0 or spin-1 bosonic mediator coupled to the initial-state particles, the DM particles leave the detector without measurable signatures. If DM particles are produced in association with a detectable SM particle, which could be emitted as initial-state radiation from the interacting constituents of the colliding protons, or through new effective couplings between DM and SM particles, their existence could be inferred via a large transverse momentum imbalance in the collision event.

The production of the SM Higgs boson [5–7] via initial-state radiation is highly suppressed because of the mass dependence of its coupling strength to fermions. Nonetheless, the associated production of a Higgs boson and DM particles can occur if the Higgs boson takes part in the interaction producing the DM particles [8–10]. Such a production mechanism would allow one to directly probe the structure of the effective DM–SM coupling.

In this paper, we present a search for DM production in association with a scalar Higgs boson, h, with a mass of 125 GeV that decays to a bottom quark–antiquark pair ($\text{b}\overline{\text{b}}$). As the $\text{b}\overline{\text{b}}$ decay mode has the largest branching fraction of all Higgs boson decay modes allowed in the SM, it provides the largest signal yield. The search is performed using the data set collected by the CMS experiment [11] at the CERN Large Hadron Collider (LHC) at a center-of-mass energy of 13 TeV in 2016, corresponding to an integrated luminosity of approximately $35.9\,\text{fb}^{-1}$. Similar searches have been conducted at the LHC by both the ATLAS and CMS Collaborations, analyzing data collected at 8 [12] and 13 TeV [13,14]. Results are interpreted in terms of two simplified models predicting this signature. The first is a type-2 two-Higgs doublet model extended by an additional light pseudoscalar boson a (2HDM+a) [15]. The a boson mixes with the scalar and pseudoscalar partners of the observed Higgs boson, and decays to a pair of DM particles, $\chi\overline{\chi}$. The second is a baryonic Z′ model [10], in which a "baryonic Higgs" boson mixes with the SM Higgs boson. In this model, a vector mediator Z′ is exchanged in the s-channel and, after the radiation of an SM Higgs boson, decays to two DM particles. Representative Feynman diagrams for the two models are presented in Fig. 1.

In the 2HDM+a model, the DM particle candidate χ is a fermion that can couple to SM particles only through a spin-0, pseudoscalar mediator. Since the couplings of the

* e-mail: cms-publication-committee-chair@cern.ch

Published online: 27 March 2019

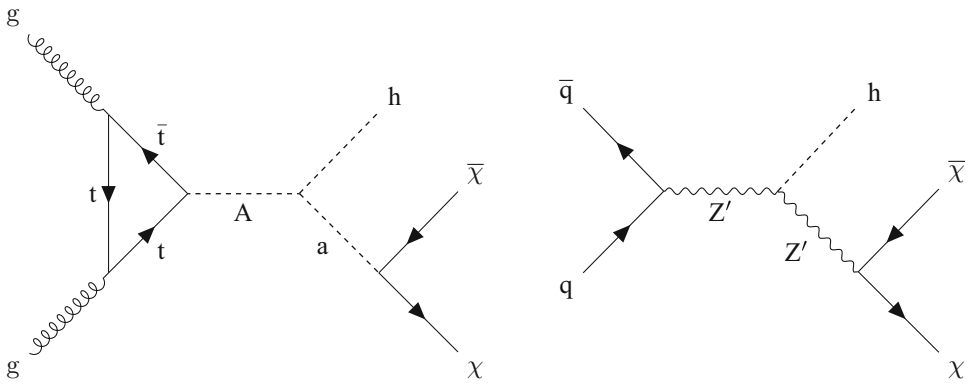

Fig. 1 Feynman diagrams for the 2HDM+a model (left) and the baryonic Z′ model (right). In both models, the scalar h can be identified with the observed 125 GeV Higgs boson

new spin-0 mediator to SM gauge bosons are strongly suppressed, the 2HDM+a model is consistent with measurements of the SM Higgs boson production and decay modes, which so far show no significant deviation from SM predictions [16]. In contrast to previously explored two-Higgs doublet models [9,12,13,17], the 2HDM+a framework ensures gauge invariance and renormalizability. In this model there are six mass eigenstates. Two are charge-parity (CP)-even scalars: the light h, assumed to be the observed 125 GeV Higgs boson, and the heavy H. These are the result of the mixing of the neutral CP-even weak eigenstates with a mixing angle α. The two CP-odd pseudoscalar mass eigenstates are the light a and the heavy A, which are linear combinations of the CP-odd weak eigenstates, with a mixing angle θ. Finally, there are two heavy charged scalars $\mathrm{H}^{\pm}$ with identical mass.

The masses of a and A, the angle θ, and the ratio of the vacuum expectation values of h and H, $\tan\beta$, are varied in this search. The mixing angle α changes with β following the relation $\alpha = \beta - \pi/2$. Perturbativity and unitarity put restrictions on the magnitudes and the signs of the three quartic couplings λ_3, λ_{P1}, λ_{P2}, and we set their values to $\lambda_3 = \lambda_{\mathrm{P1}} = \lambda_{\mathrm{P2}} = 3$ [15]. The masses of the charged Higgs bosons and of the heavy CP-even Higgs boson are assumed to be the same as the mass of the heavy pseudoscalar, i.e., $m_{\mathrm{H}} = m_{\mathrm{H}^{\pm}} = m_{\mathrm{A}}$. When performing a scan in the m_{A}-m_{a} plane, $\tan\beta$ is assumed to be 1 and $\sin\theta$ is assumed to be 0.35, following the recommendations in Ref. [18]. The DM particle χ is assumed to have a mass of $m_\chi = 10$ GeV. For $\tan\beta \gg 1$, the coupling strengths of both a and A to b quarks are enhanced, and effects from $\mathrm{b\bar{b}}$-initiated production are included in the signal simulation for all values of $\tan\beta$.

The baryonic Z′ model [10] is an extension of the SM with an additional $\mathrm{U}(1)_B$ Z′ gauge boson that couples to the baryon number B. The model predicts the existence of a new Dirac fermion that is neutral under SM gauge symmetries, has non-zero B, and is stable because of the corresponding $\mathrm{U}(1)_B$ symmetry. The state therefore serves as a good DM candidate. To generate the Z′ mass, a baryonic Higgs scalar field is introduced to spontaneously break the $\mathrm{U}(1)_B$ symmetry. In analogy with the SM, there remains a physical baryonic Higgs particle, h_B, with a vacuum expectation value v_B, which couples to the Z′ boson. The Z′ and the SM Higgs boson, h, interact with a coupling strength of $g_{\mathrm{hZ'Z'}} = m^2_{Z'} \sin\zeta / v_B$, where ζ is the h-h_B mixing angle. The chosen value for the Z′ coupling to quarks, g_{q}, is 0.25 and the Z′ coupling to DM, g_χ, is set to 1, following the recommendations in Ref. [19]. This is well below the bounds $g_{\mathrm{q}}, g_\chi \sim 4\pi$, where perturbativity and the validity of the effective field theory break down [10]. Constraints on the SM Higgs boson properties make the mixing angle ζ consistent with $\cos\zeta = 1$ within uncertainties of the order of 10%, thereby requiring $\sin\zeta$ to be less than 0.4 [10]. In this search, it is assumed that $\sin\zeta = 0.3$. It is also assumed that $g_{\mathrm{hZ'Z'}}/m_{Z'} = 1$, which implies $v_B = m_{Z'} \sin\zeta$. This choice maximizes the cross section without violating the bounds imposed by SM measurements. The free parameters in the model under these assumptions are thus $m_{Z'}$ and m_χ, which are varied in this search.

Signal events are characterized by a large imbalance in the transverse momentum (or hadronic recoil), which indicates the presence of invisible DM particles, and by hadronic activity consistent with the production of an SM Higgs boson that decays to a $\mathrm{b\bar{b}}$ pair. Thus, the search strategy followed imposes requirements on the mass of the reconstructed Higgs boson candidate, which is also required to be Lorentz-boosted. Together with the identification of the hadronization products of the two b quarks produced in the Higgs boson decay, these requirements define a data sample that is expected to be enriched in signal events. Several different SM processes can mimic this topology, the most important of which are top quark pair production and the production of a vector boson (V) in association with multiple jets. For each of these SM processes that constitute the largest sources of background, statistically independent data samples are used to predict the hadronic recoil distributions. Both the signal and background contributions to the hadronic recoil distributions observed in data are extracted with a likelihood fit, performed simultaneously in all samples.

2 The CMS detector

The CMS detector, described in detail in Ref. [11], is a multipurpose apparatus designed to study high transverse momentum (p_T) processes in proton–proton (pp) and heavy ion collisions. A superconducting solenoid occupies its central region, providing a magnetic field of 3.8 T parallel to the beam direction. Charged particle trajectories are measured using silicon pixel and strip trackers that cover a pseudorapidity region of $|\eta| < 2.5$. A lead tungstate crystal electromagnetic calorimeter (ECAL), and a brass and scintillator hadron calorimeter surround the tracking volume and extend to $|\eta| < 3$. The steel and quartz-fiber forward Cherenkov hadron calorimeter extends the coverage to $|\eta| < 5$. The muon system consists of gas-ionization detectors embedded in the steel flux-return yoke outside the solenoid and covers $|\eta| < 2.4$. Online event selection is accomplished via the two-tiered CMS trigger system [20]. The first level is designed to select events in less than 4μs, using information from the calorimeters and muon detectors. Subsequently, the high-level trigger processor farm reduces the event rate to 1 kHz.

3 Simulated data samples

The signal processes are simulated at leading order (LO) accuracy in quantum chromodynamics (QCD) perturbation theory using the MADGRAPH5_aMC@NLO v2.4.2 [21] program. To model the contributions from SM Higgs boson processes as well as from the $t\bar{t}$ and single top quark backgrounds, we use the POWHEG v2 [22–24] generator. These processes are generated at the next-to-leading order (NLO) in QCD. The $t\bar{t}$ production cross section is further corrected using calculations at the next-to-next-to-leading order in QCD including corrections for soft-gluon radiation estimated with next-to-next-to-leading logarithmic accuracy [25]. Events with multiple jets produced via the strong interaction (referred to as QCD multijet events) are generated at LO using MADGRAPH5_aMC@NLO v2.2.2 with up to four partons in the matrix element calculations. The MLM prescription [26] is used for matching these partons to parton shower jets. Simulated samples of Z+jets and W+jets processes are generated at LO using MADGRAPH5_aMC@NLO v2.3.3. Up to four additional partons are considered in the matrix element and matched to their parton showers using the MLM technique. The V+jets (V = W, Z) samples are corrected by weighting the p_T of the respective boson with NLO QCD corrections obtained from large samples of events generated with MADGRAPH5_aMC@NLO and the FxFx merging technique [27] with up to two additional jets stemming from the matrix element calculations. These samples are further corrected by applying NLO electroweak corrections [28–30] that depend on the boson p_T. Predictions for the SM diboson production modes WW, WZ, and ZZ are obtained at LO with the PYTHIA 8.205 [31] generator and normalized to NLO accuracy using MCFM v6.0 [32].

The LO or NLO NNPDF 3.0 parton distribution functions (PDFs) [33] are used, depending on the QCD order of the generator used for each physics process. Parton showering, fragmentation, and hadronization are simulated with PYTHIA 8.212 using the CUETP8M1 underlying event tune [34,35]. Interactions of the resulting final state particles with the CMS detector are simulated using the GEANT4 program [36]. Additional inelastic pp interactions in the same or a neighboring bunch crossing (pileup) are included in the simulation. The pileup distribution is adjusted to match the corresponding distribution observed in data.

4 Event reconstruction

The reconstructed interaction vertex with the largest value of summed physics-object p_T^2 is taken to be the primary event vertex. The physics objects used for the primary event vertex determination are the clusters found by the anti-k_T clustering algorithm [37,38], with a distance parameter of 0.4, from the charged particle tracks in the event, as well as the associated missing transverse momentum, taken as the negative vector sum of the p_T of those clusters. The offline selection requires all events to have a primary vertex reconstructed within a 24 cm window along the z-axis around the nominal interaction point, and a transverse distance from the nominal interaction region less than 2 cm.

The particle-flow (PF) algorithm [39] aims to reconstruct and identify each individual particle in an event, with an optimized combination of information from the various elements of the CMS detector. The energy of photons is obtained from the ECAL measurement. The energy of electrons is determined from a combination of the electron momentum at the primary interaction vertex as determined by the tracker, the energy of the corresponding ECAL cluster, and the energy sum of all bremsstrahlung photons spatially compatible with originating from the electron track. The energy of muons is obtained from the curvature of the corresponding track. The energy of charged hadrons is determined from a combination of their momentum measured in the tracker and the matching ECAL and HCAL energy deposits, corrected for zero-suppression effects and for the response function of the calorimeters to hadronic showers. Finally, the energy of neutral hadrons is obtained from the corresponding corrected ECAL and HCAL energies. The PF candidates are then used to construct the physics objects described in this section. At large Lorentz boosts, the two b quarks from the Higgs boson decay may produce jets that overlap and make their individual reconstruction difficult. In this search large-area jets

clustered from PF candidates using the Cambridge–Aachen algorithm [40] with a distance parameter of 1.5 (CA15 jets) are utilized to identify the Higgs boson candidate. The large cone size is chosen in order to select signal events where the Higgs boson has a medium Lorentz-boost and hence its decay products begin to merge for $p_{\mathrm{T}}(\mathrm{h}) \gtrsim 200\,\mathrm{GeV}$. To reduce the impact of particles arising from pileup interactions, the four-vector of each PF candidate is scaled with a weight calculated with the pileup per particle identification (PUPPI) algorithm [41] prior to the clustering. The absolute jet energy scale is corrected using calibrations derived from data [42]. The CA15 jets are also required to be central ($|\eta| < 2.4$). The "soft-drop" (SD) jet grooming algorithm [43] is applied to remove soft wide-angle radiation from the jets. We refer to the mass of the groomed CA15 jet as m_{SD}.

The ability to identify two b quarks inside a single CA15 jet is crucial for this search. A likelihood for the CA15 jet to contain two b quarks is derived by combining the information from primary and secondary vertices and tracks in a multivariate discriminant optimized to distinguish CA15 jets originating from $\mathrm{h} \to \mathrm{b\bar{b}}$ decays from the cases where the hadronization of energetic quarks or gluons [44] leads to the presence of a CA15 jet. The working point chosen for this algorithm (the "double-b tagger") corresponds to an identification efficiency of 50% for a $\mathrm{b\bar{b}}$ system with a p_{T} of 200 GeV, and a probability of 10% for misidentifying CA15 jets originating from combinations of quarks or gluons not coming from a resonance decay. The efficiency of the algorithm increases with the p_{T} of the $\mathrm{b\bar{b}}$ system, reaching an efficiency of 65% for a CA15 jet with a $p_{\mathrm{T}} > 500\,\mathrm{GeV}$. In this p_{T} regime, the misidentification rate for QCD jets is about 13%. The probability for misidentifying CA15 jets from top quark decays is 14% across the entire p_{T} spectrum. These estimates are derived with no additional requirements on the CA15 jet kinematics.

Energy correlation functions are used to identify the two-prong structure in the CA15 jet expected from a Higgs boson decay to two b quarks, and to distinguish it from QCD-like jets (i.e., jets that do not originate from a heavy resonance decay) and jets from the hadronic decays of top quarks. The energy correlation functions (${}_{v}e_{N}$) are sensitive to correlations among the constituents of the CA15 jet [45] and depend on N factors of the particle energies and v factors of their pairwise angles, weighted by the angular separation of the constituents.

As motivated in Ref. [45], the ratio $N_2 = {}_2e_3^{(\beta)}/({}_1e_2^{(\beta)})^2$ is used as a two-prong tagger for the identification of the CA15 jet containing the Higgs boson decay products. The parameter β, which controls the weighting of the angles between constituent pairs in the computation of the N_2 variable, is chosen to be 1 since this value gives the best two-prong jet identification.

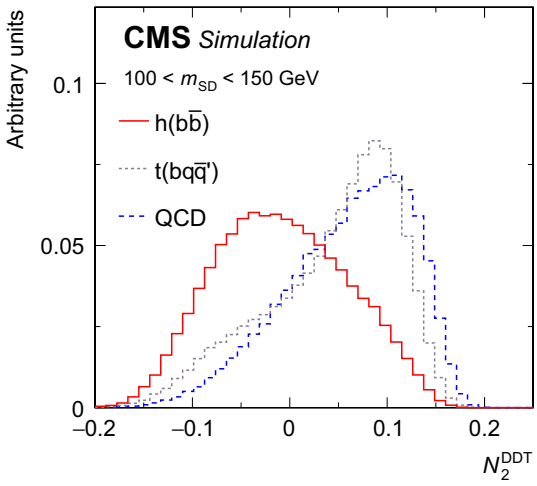

Fig. 2 The N_2^{DDT} distribution as expected for CA15 jets originating from a Higgs boson decaying to a $\mathrm{b\bar{b}}$ pair (solid red) is compared with the expected distribution for CA15 jets originating from the decay products of top quarks decaying hadronically (dotted grey). The distribution corresponding to CA15 jets that do not originate from a heavy resonance decay is also shown (dashed blue)

It is noted that requiring a jet to be two-pronged based on the value of a jet substructure variable, such as N_2, will affect the shape of the distribution of m_{SD} for the background processes. In this search, the value of m_{SD} is required to be consistent with the Higgs boson mass. It is therefore desirable to preserve a smoothly falling jet mass distribution for QCD-like jets. As motivated in Ref. [46], the dependence of N_2 on the variable $\rho = \ln(m_{\mathrm{SD}}^2/p_{\mathrm{T}}^2)$ is tested, since the distribution of ρ in QCD-like jets is expected to be invariant of the jet mass and p_{T}. The decorrelation strategy described in Ref. [46] is applied, choosing a QCD misidentification efficiency of 20%, which corresponds to a signal efficiency of 55% and a misidentification rate for top quark jets of 36% across the entire CA15 jet p_{T} spectrum. This results in a modified tagging variable, which we denote as N_2^{DDT}, where the superscript DDT stands for "designing decorrelated taggers" [46]. Figure 2 shows the expected distribution of N_2^{DDT} for CA15 jets matched to a Higgs boson decaying to a $\mathrm{b\bar{b}}$ pair, together with the distributions expected for CA15 jets matched to hadronically decaying top quarks and for QCD-like CA15 jets.

This search also utilizes narrow jets clustered from the PF candidates using the anti-k_{T} algorithm with a distance parameter of 0.4 ("AK4 jets"). Narrow jets originating from b quarks are identified using the combined secondary vertex (CSVv2) algorithm [44]. The working point used in this search has a b-jet identification efficiency of 81%, a charm jet selection efficiency of 37%, and a 9% probability of misidentifying light-flavor jets [44]. Jets that are b-tagged are required to be central ($|\eta| < 2.4$).

Electron reconstruction requires the matching of a supercluster in the ECAL with a track in the silicon tracker. Reconstructed electrons are required to be within $|\eta| < 2.5$, excluding the transition region $1.44 < |\eta| < 1.57$ between the ECAL barrel and endcap. Identification criteria [47] based on the ECAL shower shape and the consistency of the electron track with the primary vertex are imposed. Muon candidates are selected by two different reconstruction approaches [48]: one in which tracks in the silicon tracker are matched to a track segment in the muon detector, and another in which a track fit spanning the silicon tracker and muon detector is performed starting with track segments in the muon detector. Further identification criteria are imposed on muon candidates to reduce the number of hadrons and poorly measured mesons misidentified as muons [48]. These additional criteria include requirements on the number of hits in the tracker and in the muon systems, the fit quality of the global muon track, and the track's consistency with the primary vertex. Muon candidates with $|\eta| < 2.4$ are considered in this analysis. A minimum p_{T} of 10 GeV is required for electron and muon candidates. Both are required to satisfy isolation requirements that limit the total energy of tracks and calorimeter clusters measured in conical regions about them. Hadronically decaying τ leptons, τ_{had}, are reconstructed using the hadron-plus-strips algorithm [49], which uses charged hadron and neutral electromagnetic objects to reconstruct intermediate resonances into which the τ lepton decays. The τ_{had} candidates with $p_{\mathrm{T}} > 18$ GeV and $|\eta| < 2.3$ are considered [47,49,50]. Photon candidates, identified by means of requirements on the ECAL energy distribution and its distance to the closest track, must have $p_{\mathrm{T}} > 15$ GeV and $|\eta| < 2.5$.

The missing transverse momentum $\vec{p}_{\mathrm{T}}^{\,\mathrm{miss}}$ is defined as the negative vectorial sum of the p_{T} of all the reconstructed PF candidates. Its magnitude is denoted as $p_{\mathrm{T}}^{\mathrm{miss}}$. Corrections to jet momenta are propagated to the $p_{\mathrm{T}}^{\mathrm{miss}}$ calculation, and event filters are used to remove spurious high $p_{\mathrm{T}}^{\mathrm{miss}}$ events caused by instrumental noise in the calorimeters or beam halo muons [51]. These filters remove about 1% of signal events.

5 Event selection

Signal events are characterized by a high value of $p_{\mathrm{T}}^{\mathrm{miss}}$, the absence of any isolated lepton (e, μ, or τ) or photon, and the presence of a CA15 jet identified as a Higgs boson candidate. In the signal region (SR) described below, the dominant background contributions arise from Z+jets, W+jets, and $\mathrm{t\bar{t}}$ production. To predict the $p_{\mathrm{T}}^{\mathrm{miss}}$ spectra of these processes in the SR, data from different control regions (CRs) are used. Single-lepton CRs are designed to predict the $\mathrm{t\bar{t}}$ and W+jets backgrounds, while dilepton CRs predict the Z+jets background contribution. The hadronic recoil, U, serves as a proxy for the $p_{\mathrm{T}}^{\mathrm{miss}}$ distribution of the main background processes in the SR and is defined by excluding the electron(s) and muon(s) from the $p_{\mathrm{T}}^{\mathrm{miss}}$ computation in the CRs. Predictions for other backgrounds are obtained from simulation.

Events are selected online by the high level trigger system, using a jet reconstruction algorithm and constituents that mirror those of the offline analysis. The trigger requires large values of $p_{\mathrm{T,trig}}^{\mathrm{miss}}$ or $H_{\mathrm{T}}^{\mathrm{miss}}$, where $p_{\mathrm{T,trig}}^{\mathrm{miss}}$ is the magnitude of the vectorial $\vec{p}_{\mathrm{T}}$ sum over all PF particles and $H_{\mathrm{T}}^{\mathrm{miss}}$ is the magnitude of the vectorial $\vec{p}_{\mathrm{T}}$ sum over all AK4 jets with $p_{\mathrm{T}} > 20$ GeV and $|\eta| < 5.2$ at the trigger level. Muon candidates are excluded from the online $p_{\mathrm{T,trig}}^{\mathrm{miss}}$ calculation. Minimum thresholds on $p_{\mathrm{T,trig}}^{\mathrm{miss}}$ and $H_{\mathrm{T}}^{\mathrm{miss}}$ are between 90 and 120 GeV, depending on the data-taking period. Collectively, online requirements on $p_{\mathrm{T,trig}}^{\mathrm{miss}}$ and $H_{\mathrm{T}}^{\mathrm{miss}}$ are referred to as $p_{\mathrm{T}}^{\mathrm{miss}}$ triggers. These triggers are measured to be 96% efficient for $p_{\mathrm{T}}^{\mathrm{miss}}(U) > 200$ GeV and 100% efficient for $p_{\mathrm{T}}^{\mathrm{miss}}(U) > 350$ GeV. For CRs that require the presence of electrons, events are collected by single-electron triggers, in which at least one electron is required by the online selection criteria. These sets of requirements are referred to as single-electron triggers.

A common set of preselection criteria is used for all regions. The presence of exactly one CA15 jet with $p_{\mathrm{T}} > 200$ GeV and $|\eta| < 2.4$ is required. It is also required that $100 < m_{\mathrm{SD}} < 150$ GeV and $N_2^{\mathrm{DDT}} < 0$. In the SR (CRs), $p_{\mathrm{T}}^{\mathrm{miss}}$ (U) has to be larger than 200 GeV, and the minimum azimuthal angle ϕ between any AK4 jet and the direction of $\vec{p}_{\mathrm{T}}^{\,\mathrm{miss}}$ $(\vec{U})$ must be larger than 0.4 radians to reject multijet events that mimic signal events. Events with any τ_{had} candidate or photon candidate are vetoed. The number of AK4 jets for which $\Delta R = \sqrt{(\Delta\eta)^2 + (\Delta\phi)^2} > 1.5$, where $\Delta\eta$ and $\Delta\phi$ are, respectively, the differences in pseudorapidity and in the azimuthal angle (measured in radians) of a given AK4 jet and the CA15 jet, is required to be smaller than two. This number is referred to as "additional AK4 jets" in the following. This requirement significantly reduces the contribution from $\mathrm{t\bar{t}}$ events in the SR.

Events that meet the preselection criteria described above are split into the SR and the different CRs based on their lepton multiplicity and the presence of a b-tagged AK4 jet not overlapping with the CA15 jet, as summarized in Table 1. For the SR, events are selected if they have no isolated electrons (muons) with $p_{\mathrm{T}} > 10$ GeV and $|\eta| < 2.5$ (2.4), and the previously described double-b tag requirement on the Higgs boson candidate CA15 jet is imposed.

To predict the $p_{\mathrm{T}}^{\mathrm{miss}}$ spectrum of the Z+jets process in the SR, dimuon and dielectron CRs are used. Dimuon events are selected online employing the same $p_{\mathrm{T}}^{\mathrm{miss}}$ triggers that are used in the SR. These events are required to have two oppositely charged muons (having $p_{\mathrm{T}} > 20$ GeV and $p_{\mathrm{T}} > 10$ GeV for the leading and trailing muon, respec-

Table 1 Event selection criteria defining the signal and control regions. These criteria are applied in addition to the preselection common to all regions, as described in the text. The presence of a b-tagged AK4 jet that does not overlap with the CA15 jet is vetoed in all analysis regions except for the single-lepton CR enriched in $\mathrm{t\bar{t}}$ events, for which such an AK4 b tag is required

Region	Main background process	Additional AK4 b tag	Leptons	Double-b tag
Signal	Z+jets, $\mathrm{t\bar{t}}$, W+jets	0	0	Pass
Single-lepton	W+jets, $\mathrm{t\bar{t}}$	0	1	Pass/fail
Single-lepton, b-tagged	$\mathrm{t\bar{t}}$, W+jets	1	1	Pass/fail
Dilepton	Z+jets	0	2	Pass/fail

tively) with an invariant mass between 60 and 120 GeV. The leading muon has to satisfy tight identification and isolation requirements and is selected with an average efficiency of 95%. Dielectron events are selected online using single-electron triggers. Two oppositely charged electrons with p_{T} greater than 10 GeV are required offline, and they must form an invariant mass between 60 and 120 GeV. To be on the plateau of the trigger efficiency, at least one of the two electrons must have $p_{\mathrm{T}} > 40$ GeV and must satisfy tight identification and isolation requirements that correspond to an efficiency of 70% [47].

Events that satisfy the SR selection because of the loss of a single lepton primarily originate from W+jets and semileptonic $\mathrm{t\bar{t}}$ events. To predict these backgrounds, four single-lepton samples are used: single-electron and single-muon, with and without a b-tagged AK4 jet outside the CA15 jet. The single-lepton CRs with a b-tagged AK4 jet target $\mathrm{t\bar{t}}$ events, while the other two single-lepton CRs target W+jets events. Single-muon events are selected using the $p_{\mathrm{T}}^{\mathrm{miss}}$ triggers described above. Single-electron events are selected using the same single-electron triggers employed in the online selection of dielectron events. The electron (muon) candidate in these events is required to have $p_{\mathrm{T}} > 40$ (20) GeV and to satisfy tight identification and isolation requirements. In addition, samples with a single electron must have $p_{\mathrm{T}}^{\mathrm{miss}} > 50$ GeV to avoid a large contamination from multijet events.

Each CR is further split into two subsamples depending on whether or not the CA15 jet satisfies the double-b tag requirement. This division allows for an in situ calibration of the scale factor that corrects the simulated misidentification probability of the double-b tagger for the three main backgrounds to the probability observed in data.

6 Signal extraction

As mentioned in Sect. 1, signal and background contributions to the data are extracted with a simultaneous binned likelihood fit (using the RooStats package [52]) to the $p_{\mathrm{T}}^{\mathrm{miss}}$ and U distributions in the SR and the CRs. The dominant SM process in each CR is used to predict the respective background in the SR via transfer factors T. These factors are determined in simulation and are given by the ratio of the prediction for a given bin in $p_{\mathrm{T}}^{\mathrm{miss}}$ in the SR and the corresponding bin in U in the CR, for the given process. This ratio is determined independently for each bin of the corresponding distribution.

For example, if $\mathrm{b}\ell$ denotes the $\mathrm{t\bar{t}}$ process in the b-tagged single-lepton control sample that is used to estimate the $\mathrm{t\bar{t}}$ contribution in the SR, the expected number of $\mathrm{t\bar{t}}$ events, N_i, in the i^{th} bin of the SR is then given by $N_i = \mu_i^{\mathrm{t\bar{t}}} / T_i^{\mathrm{b}\ell}$, where $\mu_i^{\mathrm{t\bar{t}}}$ is a freely floating parameter included in the likelihood to scale the $\mathrm{t\bar{t}}$ contribution in bin i of U in the CR.

The transfer factors used to predict the W+jets and $\mathrm{t\bar{t}}$ backgrounds take into account the impact of lepton acceptances and efficiencies, the b tagging efficiency, and, for the single-electron control samples, the additional requirement on $p_{\mathrm{T}}^{\mathrm{miss}}$. Since the CRs with no b-tagged AK4 jets and a double-b-tagged CA15 jet also have significant contributions from the $\mathrm{t\bar{t}}$ process, transfer factors to predict this contamination from $\mathrm{t\bar{t}}$ events are also imposed between the single-lepton CRs with and without b-tagged AK4 jets. A similar approach is applied to estimate the contamination from W+jets production in the $\mathrm{t\bar{t}}$ CR with events that fail the double-b tag requirement. Likewise, the Z+jets background prediction in the signal region is connected to the dilepton CRs via transfer factors. They account for the difference in the branching fractions of the $\mathrm{Z} \to \nu\nu$ and the $\mathrm{Z} \to \ell\ell$ decays and the impacts of lepton acceptances and selection efficiencies.

7 Systematic uncertainties

Nuisance parameters are introduced into the likelihood fit to represent the systematic uncertainties of the search. They can affect either the normalization or the shape of the $p_{\mathrm{T}}^{\mathrm{miss}}$ (U) distribution for a given process in the SR (CRs) and can be constrained in the fit. The shape uncertainties are incorporated by means of Gaussian prior distributions, while the rate uncertainties are given a log-normal prior distributions. The list of the systematic uncertainties considered in this search is presented in Table 2. To better estimate their impact on the results, uncertainties from a similar source (e.g., uncertainties in the trigger efficiencies) have been grouped. The groups of uncertainties have been ordered by the improvement in sensitivity obtained by removing the corresponding

Table 2 Sources of systematic uncertainty, along with the type (rate/shape) of uncertainty and the affected processes. For the rate uncertainties, the percentage value of the prior is quoted. The last column denotes the improvement in the expected limit when removing the uncertainty group from the list of nuisances included in the likelihood fit. Such improvement is estimated considering as signal processes the 2HDM+a model with $m_A = 1.1$ TeV and $m_a = 150$ GeV and the baryonic Z′ model with $m_{Z'} = 0.2$ TeV and $m_\chi = 50$ GeV

Systematic uncertainty	Type	Processes	Impact on sensitivity	
			2HDM+a	Baryonic Z′
Double-b mistagging	Shape	Z+jets, W+jets, $t\bar{t}$	4.8%	14.8%
Transfer factor stat. uncertainties	Shape	Z+jets, W+jets, $t\bar{t}$	1.9%	4.0%
Double-b tagging	Shape	SM h, signal	1.2%	1.1%
N_2^{DDT} efficiency	7%	Diboson, SM h, signal		
CA15 jet energy	4%	Single t, diboson, multijet, SM h, signal	0.8%	0.6%
$p_{\mathrm{T}}^{\mathrm{miss}}$ magnitude	5%	All	0.7%	< 0.5%
Integrated luminosity	2.5%	Single t, diboson, multijet, SM h, signal	< 0.5%	< 0.5%
$p_{\mathrm{T}}^{\mathrm{miss}}$ trigger efficiency	Shape/rate	All	< 0.5%	< 0.5%
Single-electron trigger	1%	All		
AK4 b tagging	Shape	All	< 0.5%	< 0.5%
τ lepton veto	3%	All	< 0.5%	0.7%
Lepton efficiency	1% per lepton	All		
Renorm./fact. scales	Shape	SM h	< 0.5%	< 0.5%
PDF	Shape	SM h		
Multijet normalization	100%	Multijet		
Theoretical cross section	20%	Single t, diboson		

nuisances in the likelihood fit. The sensitivity in the baryonic Z′ model is generally poorer than that of a 2HDM+a model because the former predicts a more background-like $p_{\mathrm{T}}^{\mathrm{miss}}$ distribution. The description of each single uncertainty in the text follows the same order as in the table.

Scale factors are used to correct for differences in the double-b tagger misidentification efficiencies in data and in the simulated W/Z+jets and $t\bar{t}$ samples. These scale factors are measured by simultaneously fitting events that pass or fail the double-b tag requirement. The correlation between the double-b tagger and $p_{\mathrm{T}}^{\mathrm{miss}}$ (or U) is taken into account by allowing recoil bins to fluctuate within a constraint that depends on the recoil value. Such dependence is estimated from the profile of the two-dimensional distribution of the double-b tag discriminant vs. the p_{T} of the CA15 jet. This is the shape uncertainty that has the largest impact on the upper limits on the signal cross sections.

Shape uncertainties due to the bin-by-bin statistical uncertainties in the transfer factors are considered for the Z+jets, W+jets, and $t\bar{t}$ processes.

For the signal and the SM h processes, an uncertainty in the double-b tagging efficiency is applied that depends on the p_{T} of the CA15 jet. This shape uncertainty has been derived through a measurement performed using a sample enriched in multijet events with double-muon-tagged $g \to b\bar{b}$ splittings. A 7% rate uncertainty in the efficiency of the requirement on the substructure variable N_2^{DDT}, which is used to identify two-prong CA15 jets, is assigned to all processes where the decay of a resonance inside the CA15 jet cone is expected. Such processes include signal production together with SM h and diboson production. The uncertainty has been derived from the efficiency measurement obtained by performing a fit in a control sample enriched in semi-leptonic $t\bar{t}$ events, where the CA15 jet originates from the W boson that comes from the hadronically decaying top quark.

A 4% rate uncertainty due to the imperfect knowledge of the CA15 jet energy scale [42] is assigned to all the processes obtained from simulation.

Similarly, a 5% rate uncertainty in the $p_{\mathrm{T}}^{\mathrm{miss}}$ magnitude, as measured by CMS in Ref. [53], is assigned to each of the processes estimated from simulation.

A rate uncertainty of 2.5% in the integrated luminosity measurement [54] is included and assigned to processes determined from simulation. In these cases, uncertainties in

Table 3 Post-fit event yield expectations per $p_{\mathrm{T}}^{\mathrm{miss}}$ bin for the SM backgrounds in the signal region when including the signal region data in the likelihood fit, under the background-only assumption. Also quoted are the expected yields for two signal models. Uncertainties quoted in the predictions include both the systematic and statistical components

$p_{\mathrm{T}}^{\mathrm{miss}}$ bin	200–270 GeV	270–350 GeV	350–475 GeV	> 475 GeV
Z+jets	249 ± 22	97.2 ± 8.5	32.6 ± 3.6	11.1 ± 1.9
$\mathrm{t\bar{t}}$	199 ± 14	52.1 ± 5.2	11.1 ± 2.0	0.7 ± 0.4
W+jets	122 ± 22	45.0 ± 8.7	8.4 ± 1.9	2.9 ± 0.9
Single t	21.0 ± 4.2	6.1 ± 1.2	0.9 ± 0.2	0.2 ± 0.1
Diboson	16.0 ± 3.1	7.6 ± 1.5	2.4 ± 0.5	1.0 ± 0.2
SM h	12.6 ± 1.4	6.6 ± 0.7	3.3 ± 0.3	1.3 ± 0.1
Σ (SM)	619 ± 20	215 ± 8	58.7 ± 3.7	17.2 ± 2.0
Data	619	214	59	21
2HDM+a, $m_{\mathrm{A}} = 1$ TeV, $m_{\mathrm{a}} = 150$ GeV	5.7 ± 0.6	9.8 ± 1.1	18.5 ± 2.1	5.2 ± 0.6
Bar. Z′, $m_{Z'} = 0.2$ TeV, $m_{\chi} = 50$ GeV	184 ± 20	118 ± 13	69.5 ± 7.7	28.9 ± 3.3

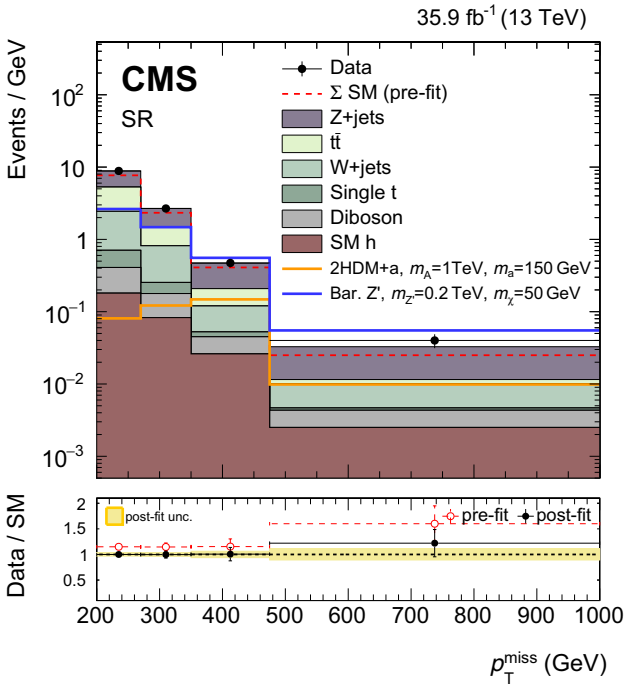

Fig. 3 The $p_{\mathrm{T}}^{\mathrm{miss}}$ distribution in the signal region before and after a likelihood fit. The data are in agreement with post-fit background predictions for the SM backgrounds, and no significant excess is observed. The dashed red histogram corresponds to the pre-fit estimate for the SM backgrounds. The lower panel shows the ratio of the data to the predicted SM background, before and after the fit. The rightmost $p_{\mathrm{T}}^{\mathrm{miss}}$ bin includes overflow events

the PDFs and uncertainties due to variations in the QCD renormalization and factorization scales are included as shape uncertainties, obtained by varying those parameters in the simulation.

The $p_{\mathrm{T}}^{\mathrm{miss}}$ trigger efficiency is parametrized as a function of U and measured using both single-muon and dimuon events. The difference between these measurements is used to derive an uncertainty, which results in a 1% rate uncertainty for processes estimated using simulation. Processes estimated using control regions ($\mathrm{t\bar{t}}$, W+jets, and Z+jets) are sensitive to the effect of this uncertainty as a function of U, so a shape uncertainty (as large as 2% at low U values) is considered for such processes. The efficiencies of the single-electron triggers are parametrized as a function of the electron p_{T} and η and an associated 1% systematic uncertainty is added into the fit.

An uncertainty in the efficiency of the CSV b tagging algorithm applied to isolated AK4 jets is assigned to the transfer factors used to predict the $\mathrm{t\bar{t}}$ background. The scale factors that correct this efficiency are measured with standard CMS methods [44]. They depend on the p_{T} and η of the b-tagged (or mistagged) jet and therefore their uncertainties are included in the fit as shape uncertainties.

The uncertainty in the τ lepton veto amounts to 3%, correlated across all U bins. Also correlated across all U bins are the uncertainties in the electron and muon selection efficiencies, which amount to 1%.

An uncertainty of 21% in the heavy-flavor fraction of W+jets is reported in previous CMS measurements [55,56]. The uncertainty in the heavy-flavor fraction of jets produced together with a Z boson is measured to be 22% [57,58]. To take into account the variation of the double-b tagging efficiency introduced by such uncertainties, the efficiencies for the W+jets and Z+jets processes are reevaluated after varying the heavy-flavor component in the simulation. The difference in the efficiency with respect to the nominal efficiency value is taken as a systematic uncertainty, and amounts to 4% in the rate of the W+jets process and 5% in the rate of the Z+jets process.

Uncertainties in the SM h production due to variations of the renormalization/factorization scales and PDFs are included as shape variations. An uncertainty of 100% is assigned to the QCD multijet yield. This uncertainty is esti-

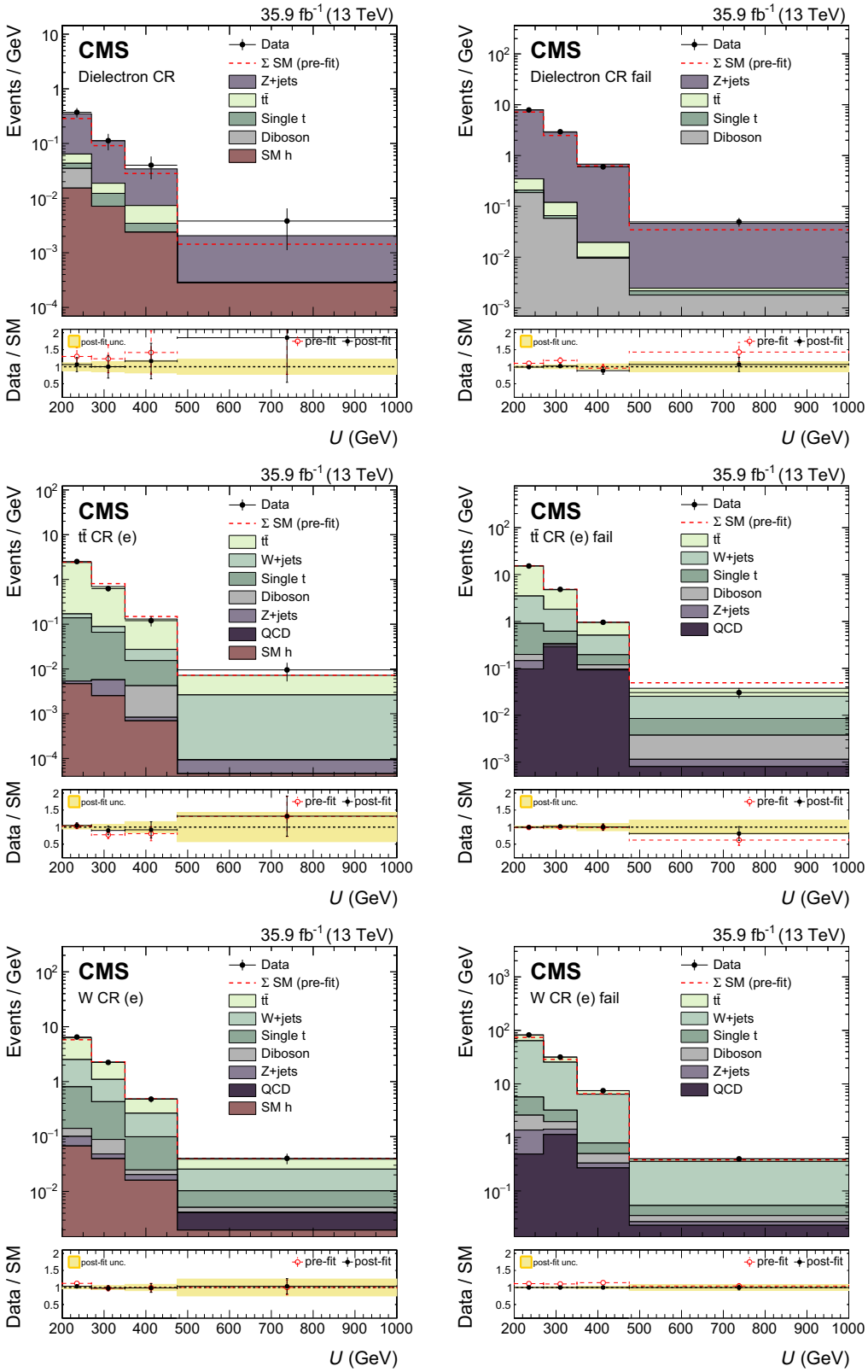

Fig. 4 The U distribution in the electron control regions before and after a background-only fit to data, including the data in the signal region in the likelihood. For the distributions on the left the CA15 jet passes the double-b tag requirement and for the distributions on the right it fails the double-b tag requirement. The lower panel shows the ratio of the data to the predicted SM background, before and after the fit. The rightmost U bin includes overflow events

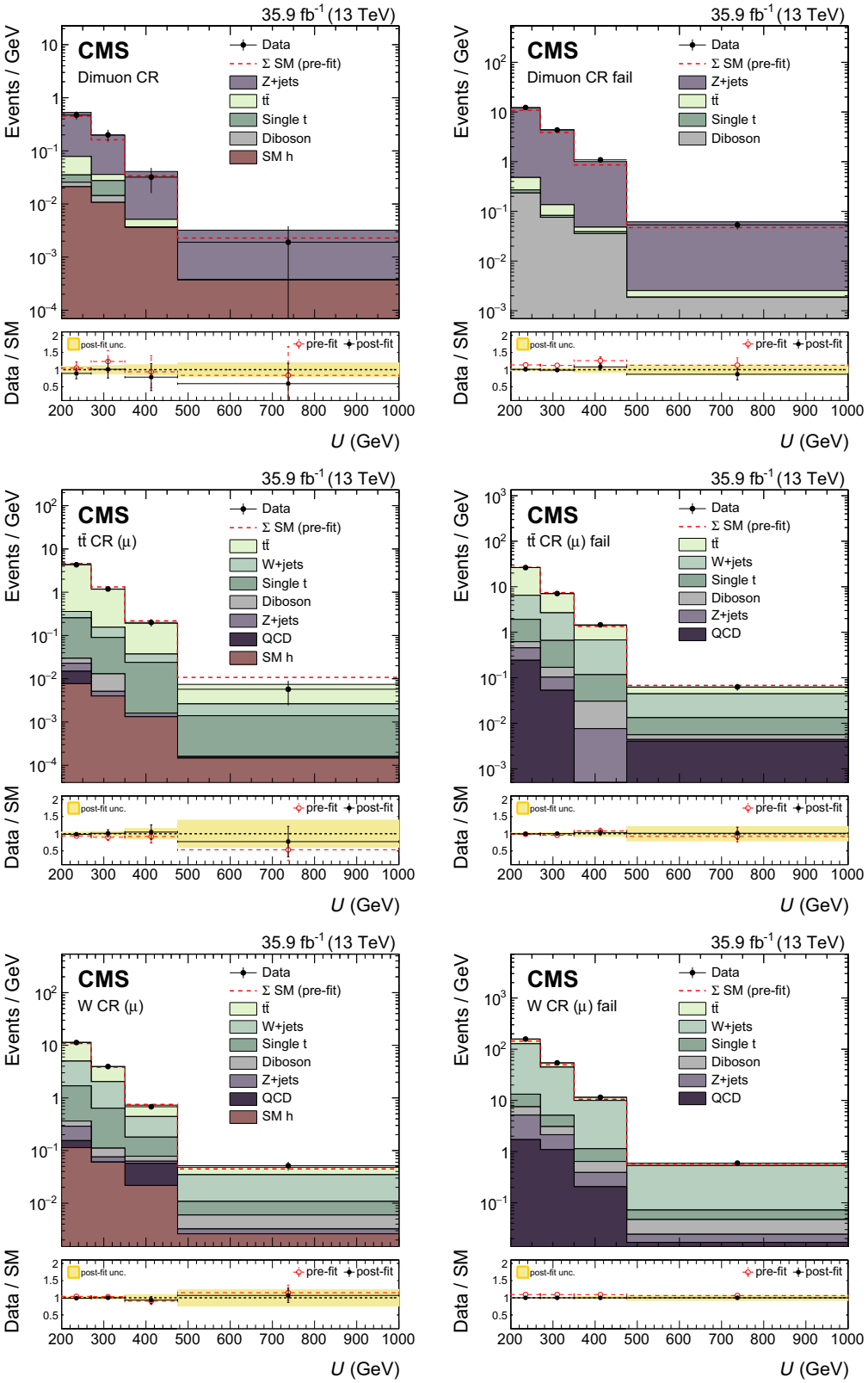

Fig. 5 The U distribution in the muon control regions before and after a background-only fit to data, including the data in the signal region in the likelihood. For the distributions on the left the CA15 jet passes the double-b tag requirement and for the distributions on the right it fails the double-b tag requirement. The lower panel shows the ratio of the data to the predicted SM background, before and after the fit. The rightmost U bin includes overflow events

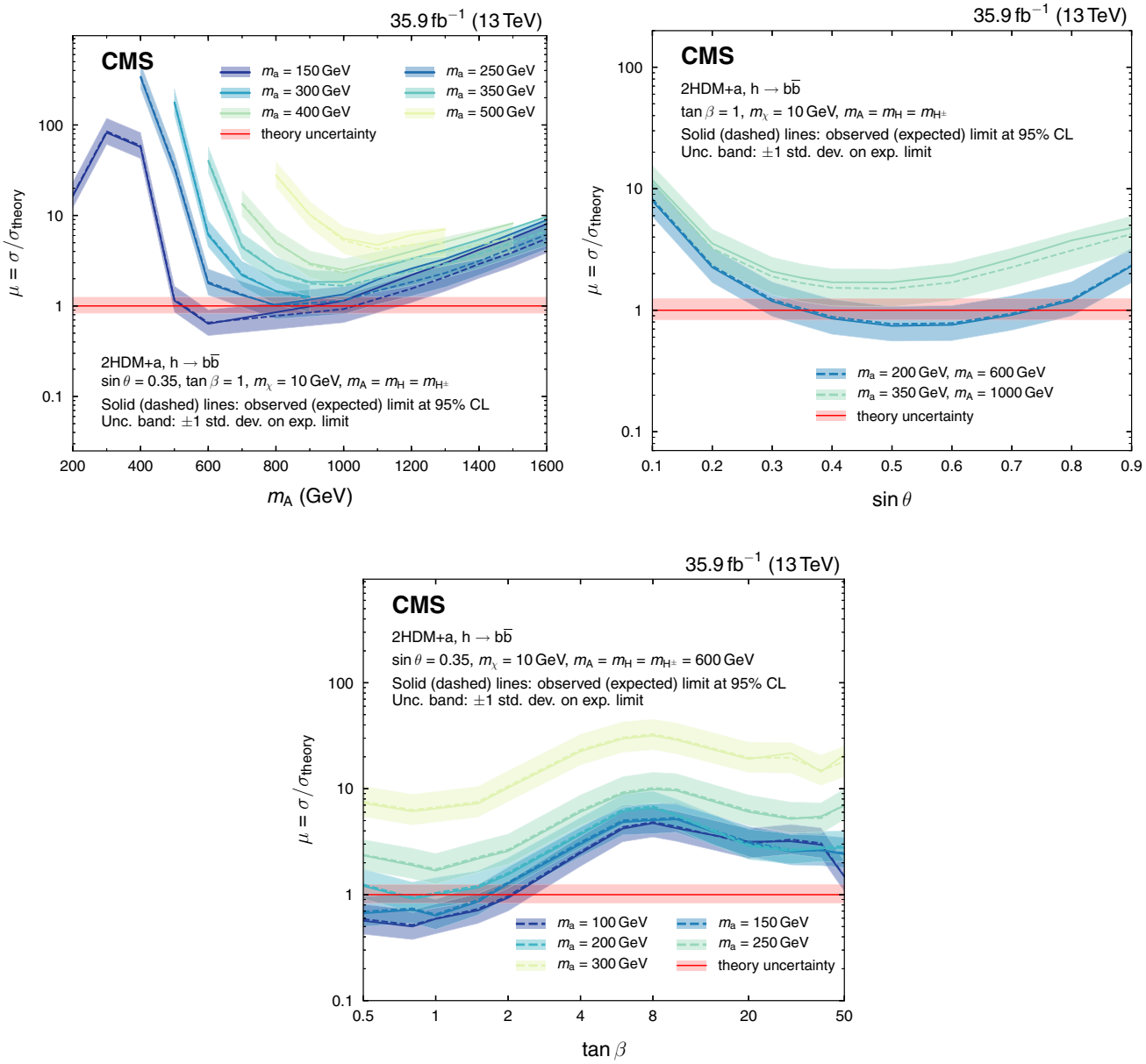

Fig. 6 Upper limits at 95% CL on the signal strength modifier, defined as $\mu = \sigma/\sigma_{\text{theory}}$, where σ_{theory} is the predicted production cross section of DM candidates in association with a Higgs boson and σ is the upper limit on the observed cross section. Limits are shown for the 2HDM+a model when scanning m_A and m_a (upper left), the mixing angle θ (upper right), or $\tan\beta$ (lower). The uncertainty in the computation of σ_{theory} is 20% and is shown as a red band around the exclusion line at $\mu = 1$

mated using a sample enriched in multijet events. The sample is obtained by vetoing leptons and photons, requiring $p_{\text{T}}^{\text{miss}} > 250$ GeV and requiring that the minimum azimuthal angle between $\vec{p}_{\text{T}}^{\text{miss}}$ and the jet directions be less than 0.1 radians. One nuisance parameter represents the uncertainty in QCD multijet yields in the signal region, while separate nuisance parameters are introduced for the muon CRs and electron CRs. A systematic uncertainty of 20% is assigned to the single top quark background yields as reported by CMS in Ref. [59] and is correlated between the SR and the CRs. An uncertainty of 20%, correlated across the SR and CRs, is also assigned to the diboson production cross section as measured by CMS in Refs. [60,61].

8 Results

The expected yields for each background in the SR and their uncertainties, as determined in the likelihood fit under the background-only assumption, are presented in Table 3, along with the observed data yields. Good agreement is observed between data and the predictions. Due to anticorrelations

between background processes, in some bins the uncertainty in the background sum is smaller than the uncertainties in the individual contributions, such as, for example, the Z+jets yields.

Expected yields are also presented for two signal models. The selection efficiencies for the chosen points correspond to 5% for the 2HDM+a model and 1% for the baryonic Z′ model.

Figure 3 shows the pre-fit and post-fit $p_{\mathrm{T}}^{\mathrm{miss}}$ distributions in the SR for signal and for all SM backgrounds, as well as the observed data distribution. The likelihood fit has been performed simultaneously in all analysis regions. The data agree with the background predictions at the one standard deviation level, and the post-fit estimate of the SM background is slightly larger than the pre-fit one. The distributions for U in the muon and electron CRs, after a fit to the data, are presented in Figs. 4 and 5.

No significant excess over the SM background expectation is observed in the SR. The results of this search are interpreted in terms of upper limits on the signal strength modifier $\mu = \sigma/\sigma_{\mathrm{theory}}$, where σ_{theory} is the predicted production cross section of DM candidates in association with a Higgs boson and σ is the upper limit on the observed cross section. The upper limits are calculated at 95% confidence level (CL) using a modified frequentist method [62–64] computed with an asymptotic approximation [65].

Figure 6 shows the upper limits on μ for the three scans (m_{A}, $\sin\theta$, and $\tan\beta$) performed. For the 2HDM+a model, m_{A} masses are excluded between 500 and 900 GeV for $m_{\mathrm{a}} = 150$ GeV, $\sin\theta = 0.35$ and $\tan\beta = 1$. Mixing angles with $0.35 < \sin\theta < 0.75$ are excluded for $m_{\mathrm{A}} = 600$ GeV and $m_{\mathrm{a}} = 200$ GeV, assuming $\tan\beta = 1$. Also excluded are $\tan\beta$ values between 0.5 and 2.0 (1.6) for $m_{\mathrm{a}} = 100$ (150) GeV and $m_{\mathrm{A}} = 600$ GeV, given $\sin\theta = 0.35$. These are the first experimental limits on the 2HDM+a model.

Figure 7 shows the expected and observed exclusion range as a function of m'_{Z} and m_χ for the baryonic Z′ model. For a DM mass of 1 GeV, masses $m_{\mathrm{Z}'} < 1.6$ TeV are excluded. The expected exclusion boundary is 1.85 TeV. Masses for the DM particles of up to 430 GeV are excluded for a 960 GeV Z′ mass. These are the most stringent limits on this model so far.

To compare results with DM direct detection experiments, limits from the baryonic Z′ model are presented in terms of a spin-independent (SI) cross section σ_{SI} for DM scattering off a nucleus. Following the recommendation of Ref. [66], the value of σ_{SI} is determined by the equation:

$$\sigma_{\mathrm{SI}} = \frac{f^2(g_{\mathrm{q}})\, g_\chi^2\, \mu_{\mathrm{n}\chi}^2}{\pi\, m_{\mathrm{med}}^4}, \tag{1}$$

where $\mu_{\mathrm{n}\chi}$ is the reduced mass of the DM-nucleon system, $f(g_{\mathrm{q}})$ is the mediator-nucleon coupling, which depends on the mediator coupling to SM quarks g_{q}, g_χ is the mediator coupling to SM particles, and m_{med} is the mass of the mediator. The resulting σ_{SI} limits as a function of the DM mass are shown in Fig. 8. Under the assumptions made for the baryonic Z′ model, these limits on the DM-nucleon SI cross section are the most stringent to date for $m_\chi < 5$ GeV.

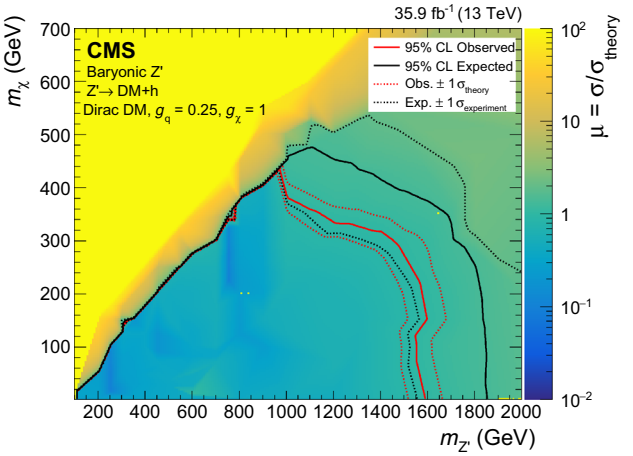

Fig. 7 Upper limits at 95% CL on the signal strength modifier, defined as $\mu = \sigma/\sigma_{\mathrm{theory}}$, where σ_{theory} is the predicted production cross section of DM candidates in association with a Higgs boson and σ is the upper limit on the observed cross section. Limits are shown for the baryonic Z′ model as a function of $m_{Z'}$ and m_χ. Mediators of up to 1.6 TeV are excluded for a DM mass of 1 GeV. Masses of the DM particle itself are excluded up to 430 GeV for a Z′ mass of 960 GeV

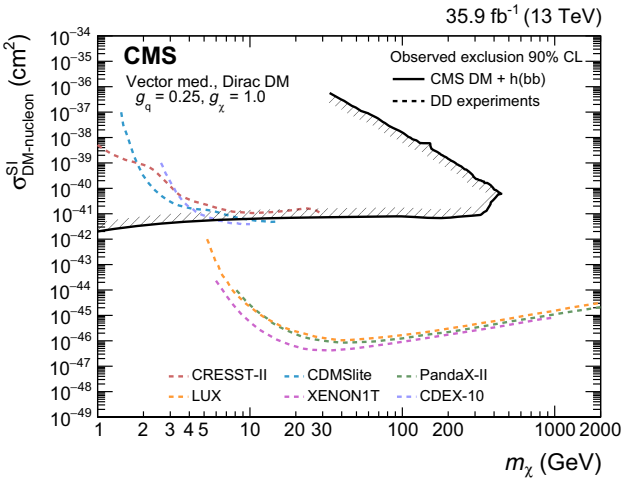

Fig. 8 The 90% CL exclusion limits on the DM-nucleon SI scattering cross section as a function of m_χ. Results for the baryonic Z′ model obtained in this analysis are compared with those from a selection of direct detection (DD) experiments. The latter exclude the regions above the curves. Limits from CRESST-II [67], CDMSlite [68], LUX [69], XENON-1T [70], PandaX-II [71], and CDEX-10 [72] are shown

9 Summary

A search for dark matter (DM) produced in association with a Higgs boson decaying to a pair of bottom quarks in a sample of proton–proton collision data corresponding to 35.9 fb^{-1} is presented. No significant deviation from the predictions of the standard model is observed, and 95% CL upper limits on the production cross sections predicted by a type-2 two-Higgs doublet model extended by an additional light pseudoscalar boson a (2HDM+a) and by the baryonic Z′ model are established. These limits constitute the most stringent exclusions from collider experiments placed on the parameters of these models to date. The 2HDM+a model is probed experimentally for the first time. For the nominal choice of the mixing angles $\sin\theta$ and $\tan\beta$ in the 2HDM+a model, the search excludes masses $500 < m_{\text{A}} < 900\,\text{GeV}$ (where A is the heavy pseudoscalar boson) assuming $m_{\text{a}} = 150\,\text{GeV}$. Scanning over $\sin\theta$ with $\tan\beta = 1$, we exclude $0.35 < \sin\theta < 0.75$ for $m_{\text{A}} = 600\,\text{GeV}$ and $m_{\text{a}} = 200\,\text{GeV}$. Finally, $\tan\beta$ values between 0.5 and 2.0 (1.6) are excluded for $m_{\text{A}} = 600\,\text{GeV}$ and $m_{\text{a}} = 100\,(150)\,\text{GeV}$ and $\sin\theta = 0.35$. In all 2HDM+a interpretations, a DM mass of $m_\chi = 10\,\text{GeV}$ is assumed. For the baryonic Z′ model, we exclude Z′ boson masses up to 1.6 TeV for a DM mass of 1 GeV, and DM masses up to 430 GeV for a Z′ boson mass of 960 GeV. The reinterpretation of the results for the baryonic Z′ model in terms of an SI nucleon scattering cross section yields a higher sensitivity for $m_\chi < 5\,\text{GeV}$ than existing results from direct detection experiments, under the assumptions imposed by the model.

Acknowledgements We congratulate our colleagues in the CERN accelerator departments for the excellent performance of the LHC and thank the technical and administrative staffs at CERN and at other CMS institutes for their contributions to the success of the CMS effort. In addition, we gratefully acknowledge the computing centers and personnel of the Worldwide LHC Computing Grid for delivering so effectively the computing infrastructure essential to our analyses. Finally, we acknowledge the enduring support for the construction and operation of the LHC and the CMS detector provided by the following funding agencies: BMBWF and FWF (Austria); FNRS and FWO (Belgium); CNPq, CAPES, FAPERJ, FAPERGS, and FAPESP (Brazil); MES (Bulgaria); CERN; CAS, MoST, and NSFC (China); COLCIENCIAS (Colombia); MSES and CSF (Croatia); RPF (Cyprus); SENESCYT (Ecuador); MoER, ERC IUT, and ERDF (Estonia); Academy of Finland, MEC, and HIP (Finland); CEA and CNRS/IN2P3 (France); BMBF, DFG, and HGF (Germany); GSRT (Greece); NKFIA (Hungary); DAE and DST (India); IPM (Iran); SFI (Ireland); INFN (Italy); MSIP and NRF (Republic of Korea); MES (Latvia); LAS (Lithuania); MOE and UM (Malaysia); BUAP, CINVESTAV, CONACYT, LNS, SEP, and UASLP-FAI (Mexico); MOS (Montenegro); MBIE (New Zealand); PAEC (Pakistan); MSHE and NSC (Poland); FCT (Portugal); JINR (Dubna); MON, RosAtom, RAS, RFBR, and NRC KI (Russia); MESTD (Serbia); SEIDI, CPAN, PCTI, and FEDER (Spain); MOSTR (Sri Lanka); Swiss Funding Agencies (Switzerland); MST (Taipei); ThEPCenter, IPST, STAR, and NSTDA (Thailand); TUBITAK and TAEK (Turkey); NASU and SFFR (Ukraine); STFC (United Kingdom); DOE and NSF (USA). Individuals have received support from the Marie-Curie program and the European Research Council and Horizon 2020 Grant, contract No. 675440 (European Union); the Leventis Foundation; the A. P. Sloan Foundation; the Alexander von Humboldt Foundation; the Belgian Federal Science Policy Office; the Fonds pour la Formation à la Recherche dans l'Industrie et dans l'Agriculture (FRIA-Belgium); the Agentschap voor Innovatie door Wetenschap en Technologie (IWT-Belgium); the F.R.S.-FNRS and FWO (Belgium) under the "Excellence of Science-EOS"—be.h project n. 30820817; the Ministry of Education, Youth and Sports (MEYS) of the Czech Republic; the Lendület ("Momentum") Program and the János Bolyai Research Scholarship of the Hungarian Academy of Sciences, the New National Excellence Program ÚNKP, the NKFIA research grants 123842, 123959, 124845, 124850 and 125105 (Hungary); the Council of Science and Industrial Research, India; the HOMING PLUS program of the Foundation for Polish Science, cofinanced from European Union, Regional Development Fund, the Mobility Plus program of the Ministry of Science and Higher Education, the National Science Center (Poland), contracts Harmonia 2014/14/M/ST2/00428, Opus 2014/13/B/ST2/02543, 2014/15/B/ST2/03998, and 2015/19/B/ST2/02861, Sonata-bis 2012/07/E/ST2/01406; the National Priorities Research Program by Qatar National Research Fund; the Programa Estatal de Fomento de la Investigación Científica y Técnica de Excelencia María de Maeztu, grant MDM-2015-0509 and the Programa Severo Ochoa del Principado de Asturias; the Thalis and Aristeia programs cofinanced by EU-ESF and the Greek NSRF; the Rachadapisek Sompot Fund for Postdoctoral Fellowship, Chulalongkorn University and the Chulalongkorn Academic into Its 2nd Century Project Advancement Project (Thailand); the Welch Foundation, contract C-1845; and the Weston Havens Foundation (USA).

Data Availability Statement This manuscript has no associated data or the data will not be deposited. [Authors' comment: Release and preservation of data used by the CMS Collaboration as the basis for publications is guided by the CMS policy as written in its document "CMS data preservation, re-use and open access policy" (https://cmsdocdb.cern.ch/cgibin/PublicDocDB/RetrieveFile?docid=6032&filename=CMSDataPolicyV1.2.pdf&version=2).]

Funded by SCOAP[3].

References

1. G. Bertone, D. Hooper, J. Silk, Particle dark matter: evidence, candidates and constraints. Phys. Rep. **405**, 279 (2005). https://doi.org/10.1016/j.physrep.2004.08.031. arXiv:hep-ph/0404175
2. J.L. Feng, Dark matter candidates from particle physics and methods of detection. Ann. Rev. Astron. Astrophys. **48**, 495 (2010). https://doi.org/10.1146/annurev-astro-082708-101659. arXiv:1003.0904
3. T.A. Porter, R.P. Johnson, P.W. Graham, Dark matter searches with astroparticle data. Ann. Rev. Astron. Astrophys. **49**, 155 (2011). https://doi.org/10.1146/annurev-astro-081710-102528. arXiv:1104.2836
4. Planck Collaboration, Planck 2015 results. XIII. Cosmological parameters. Astron. Astrophys. **594**, A13 (2016). https://doi.org/10.1051/0004-6361/201525830, arXiv:1502.01589
5. ATLAS Collaboration, Observation of a new particle in the search for the standard model Higgs boson with the ATLAS detector at

the LHC. Phys. Lett. B **716**, 1 (2012). https://doi.org/10.1016/j.physletb.2012.08.020, arXiv:1207.7214
6. CMS Collaboration, Observation of a new boson at a mass of 125 GeV with the CMS experiment at the LHC. Phys. Lett. B **716**, 30 (2012). https://doi.org/10.1016/j.physletb.2012.08.021. arXiv:1207.7235
7. CMS Collaboration, Observation of a new boson with mass near 125 GeV in pp collisions at $\sqrt{s} = 7$ and 8 TeV. JHEP **06**, 81 (2013). https://doi.org/10.1007/JHEP06(2013)081. arXiv:1303.4571
8. A.A. Petrov, W. Shepherd, Searching for dark matter at LHC with mono-Higgs production. Phys. Lett. B **730**, 178 (2014). https://doi.org/10.1016/j.physletb.2014.01.051. arXiv:1311.1511
9. A. Berlin, T. Lin, L.-T. Wang, Mono-Higgs detection of dark matter at the LHC. JHEP **06**, 078 (2014). https://doi.org/10.1007/JHEP06(2014)078. arXiv:1402.7074
10. L. Carpenter et al., Mono-Higgs-boson: a new collider probe of dark matter. Phys. Rev. D **89**, 075017 (2014). https://doi.org/10.1103/PhysRevD.89.075017. arXiv:1312.2592
11. CMS Collaboration, The CMS experiment at the CERN LHC. JINST **3**, 08004 (2008). https://doi.org/10.1088/1748-0221/3/08/S08004
12. ATLAS Collaboration, Search for dark matter in events with missing transverse momentum and a Higgs boson decaying to two photons in pp collisions at $\sqrt{s} = 8$ TeV with the ATLAS detector. Phys. Rev. Lett. **115**, 131801 (2015). https://doi.org/10.1103/PhysRevLett.115.131801
13. ATLAS Collaboration, Search for dark matter produced in association with a Higgs boson decaying to $b\bar{b}$ using 36 fb^{-1} of pp collisions at $\sqrt{s} = 13$ TeV with the ATLAS detector. Phys. Rev. Lett. **119**, 181804 (2017). https://doi.org/10.1103/PhysRevLett.119.181804
14. CMS Collaboration, Search for heavy resonances decaying into a vector boson and a Higgs boson in final states with charged leptons, neutrinos and b quarks at $\sqrt{s} = 13$ TeV. (2018). arXiv:1807.02826 **(submitted to JHEP)**
15. M. Bauer, U. Haisch, F. Kahlhoefer, Simplified dark matter models with two Higgs doublets: I. Pseudoscalar mediators. JHEP **05**, 138 (2017). https://doi.org/10.1007/JHEP05(2017)138. arXiv:1701.07427
16. ATLAS and CMS Collaborations, Measurements of the Higgs boson production and decay rates and constraints on its couplings from a combined ATLAS and CMS analysis of the LHC pp collision data at $\sqrt{s} = 7$ and 8 TeV. JHEP **08**, 045 (2016). https://doi.org/10.1007/JHEP08(2016)045. arXiv:1606.02266
17. CMS Collaboration, Search for associated production of dark matter with a Higgs boson decaying to $b\bar{b}$ or $\gamma\gamma$ at $\sqrt{s} = 13$ TeV. JHEP **10**, 180 (2017). https://doi.org/10.1007/JHEP10(2017)180. arXiv:1703.05236
18. LHC Dark Matter Working Group Collaboration, LHC dark matter working group: next-generation spin-0 dark matter models. (2018). arXiv:1810.09420
19. D. Abercrombie et al., Dark matter benchmark models for early LHC run-2 searches: report of the ATLAS/CMS dark matter forum. (2015). arXiv:1507.00966
20. CMS Collaboration, The CMS trigger system. JINST **12** P01020, https://doi.org/10.1088/1748-0221/12/01/P01020, arXiv:1609.02366
21. J. Alwall et al., The automated computation of tree-level and next-to-leading order differential cross sections, and their matching to parton shower simulations. JHEP **07**, 079 (2014). https://doi.org/10.1007/JHEP07(2014)079. arXiv:1405.0301
22. P. Nason, A new method for combining NLO QCD with shower Monte Carlo algorithms. JHEP **11**, 040 (2004). https://doi.org/10.1088/1126-6708/2004/11/040. arXiv:hep-ph/0409146
23. S. Frixione, P. Nason, C. Oleari, Matching NLO QCD computations with parton shower simulations: the POWHEG method. JHEP **11**, 070 (2007). https://doi.org/10.1088/1126-6708/2007/11/070. arXiv:0709.2092
24. S. Alioli, P. Nason, C. Oleari, E. Re, A general framework for implementing NLO calculations in shower Monte Carlo programs: the POWHEG BOX. JHEP **06**, 043 (2010). https://doi.org/10.1007/JHEP06(2010)043. arXiv:1002.2581
25. M. Czakon, P. Fiedler, A. Mitov, Total top-quark pair-production cross section at hadron colliders through $o(\alpha_s^4)$. Phys. Rev. Lett. **110**, 252004 (2013). https://doi.org/10.1103/PhysRevLett.110.252004. arXiv:1303.6254
26. M.L. Mangano, M. Moretti, F. Piccinini, M. Treccani, Matching matrix elements and shower evolution for top-quark production in hadronic collisions. JHEP **01**, 013 (2007). https://doi.org/10.1088/1126-6708/2007/01/013. arXiv:hep-ph/0611129
27. R. Frederix, S. Frixione, Merging meets matching in MC@NLO. JHEP **12**, 061 (2012). https://doi.org/10.1007/JHEP12(2012)061. arXiv:1209.6215
28. J.H. Kuhn, A. Kulesza, S. Pozzorini, M. Schulze, Electroweak corrections to hadronic photon production at large transverse momenta. JHEP **03**, 059 (2006). https://doi.org/10.1088/1126-6708/2006/03/059. arXiv:hep-ph/0508253
29. S. Kallweit et al., NLO QCD+EW automation and precise predictions for V+multijet production, in *50th Rencontres de Moriond on QCD and High Energy Interactions La Thuile, Italy, March 21–28, 2015*. (2015). arXiv:1505.05704
30. S. Kallweit et al., NLO QCD+EW predictions for V+jets including off-shell vector-boson decays and multijet merging. JHEP **04**, 021 (2016). https://doi.org/10.1007/JHEP04(2016)021. arXiv:1511.08692
31. T. Sjöstrand et al., An Introduction to PYTHIA 8.2. Comput. Phys. Commun. **191**, 159 (2015). https://doi.org/10.1016/j.cpc.2015.01.024. arXiv:1410.3012
32. J.M. Campbell, R.K. Ellis, C. Williams, Vector boson pair production at the LHC. JHEP **07**, 018 (2011). https://doi.org/10.1007/JHEP07(2011)018. arXiv:1105.0020
33. NNPDF Collaboration, Parton distributions for the LHC Run II. JHEP **04**, 040 (2015). https://doi.org/10.1007/JHEP04(2015)040, arXiv:1410.8849
34. CMS Collaboration, Event generator tunes obtained from underlying event and multiparton scattering measurements. Eur. Phys. J. C **76**, 155 (2016). https://doi.org/10.1140/epjc/s10052-016-3988-x. arXiv:1512.00815
35. P. Skands, S. Carrazza, J. Rojo, Tuning PYTHIA 8.1: the Monash 2013 tune. Eur. Phys. J. C **74**, 3024 (2014). https://doi.org/10.1140/epjc/s10052-014-3024-y. arXiv:1404.5630
36. GEANT4 Collaboration, GEANT4–a simulation toolkit. Nucl. Instrum. Meth. A **506**, 250 (2003). https://doi.org/10.1016/S0168-9002(03)01368-8
37. M. Cacciari, G.P. Salam, G. Soyez, The anti-k_T jet clustering algorithm. JHEP **04**, 063 (2008). https://doi.org/10.1088/1126-6708/2008/04/063. arXiv:0802.1189
38. M. Cacciari, G.P. Salam, G. Soyez, FastJet user manual. Eur. Phys. J. C **72**, 1896 (2012). https://doi.org/10.1140/epjc/s10052-012-1896-2. arXiv:1111.6097
39. CMS Collaboration, Particle-flow reconstruction and global event description with the CMS detector. JINST **12**, 10003 (2017). https://doi.org/10.1088/1748-0221/12/10/P10003. arXiv:1706.04965
40. CMS Collaboration, A Cambridge–Aachen (C–A) based jet algorithm for boosted top-jet tagging. CMS Physics Analysis Summary CMS-PAS-JME-09-001 (2009)
41. D. Berteloni, P. Harris, M. Low, N. Tran, Pileup per particle identification. JHEP **59**, 059 (2014). https://doi.org/10.1007/JHEP10(2014)059. arXiv:1407.6013
42. CMS Collaboration, Jet energy scale and resolution in the CMS experiment in pp collisions at 8 TeV. JINST **12**,

02014 (2017). https://doi.org/10.1088/1748-0221/12/02/P02014. arXiv:1607.03663
43. A.J. Larkoski, S. Marzani, G. Soyez, J. Thaler, Soft drop. JHEP **05**, 146 (2014). https://doi.org/10.1007/JHEP05(2014)146. arXiv:1402.2657
44. CMS Collaboration, Identification of heavy-flavour jets with the CMS detector in pp collisions at 13 TeV. JINST **13**, 05011 (2018). https://doi.org/10.1088/1748-0221/13/05/P05011. arXiv:1712.07158
45. I. Moult, L. Necib, J. Thaler, New angles on energy correlation functions. JHEP **12**, 153 (2016). https://doi.org/10.1007/JHEP12(2016)153. arXiv:1609.07483
46. J. Dolen et al., Thinking outside the ROCs: designing decorrelated taggers (DDT) for jet substructure. JHEP **05**, 156 (2016). https://doi.org/10.1007/JHEP05(2016)156. arXiv:1603.00027
47. CMS Collaboration, Performance of electron reconstruction and selection with the CMS detector in proton-proton collisions at $\sqrt{s} = 8$ tev. JINST **10**, 06005 (2015). https://doi.org/10.1088/1748-0221/10/06/P06005. arXiv:1502.02701
48. CMS Collaboration, Performance of CMS muon reconstruction in pp collision events at $\sqrt{s} = 7$ TeV. JINST **7**, 10002 (2012). https://doi.org/10.1088/1748-0221/7/10/P10002. arXiv:1206.4071
49. CMS Collaboration, Reconstruction and identification of τ lepton decays to hadrons and ν_τ at CMS. JINST **11**, 01019 (2016). https://doi.org/10.1088/1748-0221/11/01/P01019. arXiv:1510.07488
50. CMS Collaboration, Performance of the CMS muon detector and muon reconstruction with proton-proton collisions $\sqrt{s} = 13$ TeV. JINST **13**, 06015 (2018). https://doi.org/10.1088/1748-0221/13/06/P06015. arXiv:1804.04528
51. CMS Collaboration, Performance of missing energy reconstruction in 13 TeV pp collision data using the CMS detector. CMS Physics Analysis Summary CMS-PAS-JME-16-004 (2016)
52. L. Moneta et al., The RooStats Project, in *13th International Workshop on Advanced Computing and Analysis Techniques in Physics Research (ACAT2010)*)SISSA, 2010). arXiv:1009.1003
53. CMS Collaboration, Performance of the CMS missing transverse momentum reconstruction in pp data at $\sqrt{s} = 8$ TeV. JINST **10**, 02006 (2015). https://doi.org/10.1088/1748-0221/10/02/P02006. arXiv:1411.0511
54. CMS Collaboration, CMS luminosity measurements for the 2016 data taking period. CMS Physics Analysis Summary CMS-PAS-LUM-17-001 (2017)
55. CMS Collaboration, Differential cross section measurements for the production of a W boson in association with jets in proton-proton collisions at $\sqrt{s} = 7$ TeV. Phys. Lett. B **741**, 12 (2015). https://doi.org/10.1016/j.physletb.2014.12.003. arXiv:1406.7533
56. CMS Collaboration, Measurement of the production cross section for a W boson and two b jets in pp collisions at $\sqrt{s} = 7$ TeV. Phys. Lett. B **735**, 204 (2014). https://doi.org/10.1016/j.physletb.2014.06.041. arXiv:1312.6608
57. CMS Collaboration, Measurements of jet multiplicity and differential production cross sections of Z+jets events in proton-proton collisions at $\sqrt{s} = 7$ TeV. Phys. Rev. D **91**, 052008 (2015). https://doi.org/10.1103/PhysRevD.91.052008. arXiv:1408.3104
58. CMS Collaboration, Measurement of the production cross sections for a Z boson and one or more b jets in pp collisions at $\sqrt{s} = 7$ TeV. JHEP **06**, 120 (2014). https://doi.org/10.1007/JHEP06(2014)120. arXiv:1402.1521
59. CMS Collaboration, Observation of the associated production of a single top quark and a W boson in pp collisions at $\sqrt{s} = 8$ TeV. Phys. Rev. Lett. **112**, 231802 (2014). https://doi.org/10.1103/PhysRevLett.112.231802. arXiv:1401.2942
60. CMS Collaboration, Measurement of the ZZ production cross section and $Z \to \ell^+\ell^-\ell'^+\ell'^-$ branching fraction in pp collisions at $\sqrt{s} = 13$ TeV. Phys. Lett. B **763**, 280 (2016). https://doi.org/10.1016/j.physletb.2016.10.054. arXiv:1607.08834
61. CMS Collaboration, Measurement of the WZ production cross section in pp collisions at $\sqrt{s} = 13$ TeV. Phys. Lett. B **766**, 268 (2017). https://doi.org/10.1016/j.physletb.2017.01.011. arXiv:1607.06943
62. S. Heinemeyer et al., Handbook of LHC Higgs cross sections: 3. Higgs properties. CERN Report CERN-2013-004, (2013). https://doi.org/10.5170/CERN-2013-004, arXiv:1307.1347
63. A.L. Read, Presentation of search results: the CL_s technique. J. Phys. G **28**, 2693 (2002). https://doi.org/10.1088/0954-3899/28/10/313
64. T. Junk, Confidence level computation for combining searches with small statistics. Nucl. Instrum. Methods A **434**, 435 (1999). https://doi.org/10.1016/S0168-9002(99)00498-2. arXiv:hep-ex/9902006
65. G. Cowan, K. Cranmer, E. Gross, O. Vitells, Asymptotic formulae for likelihood-based tests of new physics. Eur. Phys. J. C **71**, 1554 (2011). https://doi.org/10.1140/epjc/s10052-011-1554-0. arXiv:1007.1727 [Erratum: https://doi.org/10.1140/epjc/s10052-013-2501-z]
66. A. Boveia et al., Recommendations on presenting LHC searches for missing transverse energy signals using simplified s-channel models of dark matter. (2016). arXiv:1603.04156
67. CRESST-II Collaboration, Results on light dark matter particles with a low-threshold CRESST-II detector. Eur. Phys. J. C **76**, 25 (2016). https://doi.org/10.1140/epjc/s10052-016-3877-3, arXiv:1509.01515
68. SuperCDMS Collaboration, New results from the search for low-mass weakly interacting massive particles with the CDMS low ionization threshold experiment. Phys. Rev. Lett. **116**, 071301 (2016). https://doi.org/10.1103/PhysRevLett.116.071301. arXiv:1509.02448
69. LUX Collaboration, Results from a search for dark matter in the complete LUX exposure. Phys. Rev. Lett. **118**, 021303 (2017). https://doi.org/10.1103/PhysRevLett.118.021303. arXiv:1608.07648
70. XENON Collaboration, First dark matter search results from the XENON1T experiment. Phys. Rev. Lett. **119**, 181301 (2017). https://doi.org/10.1103/PhysRevLett.119.181301, arXiv:1705.06655
71. PandaX-II Collaboration, Dark matter results from 54-ton-day exposure of PandaX-II experiment. Phys. Rev. Lett. **119**, 181302 (2017). https://doi.org/10.1103/PhysRevLett.119.181302. arXiv:1708.06917
72. CDEX Collaboration, Limits on light weakly interacting massive particles from the first 102.8 kg $\times$ day data of the CDEX-10 experiment. Phys. Rev. Lett. **120**, 241301 (2018). https://doi.org/10.1103/PhysRevLett.120.241301, arXiv:1802.09016

CMS Collaboration

Yerevan Physics Institute, Yerevan, Armenia
A. M. Sirunyan, A. Tumasyan

Institut für Hochenergiephysik, Wien, Austria
W. Adam, F. Ambrogi, E. Asilar, T. Bergauer, J. Brandstetter, M. Dragicevic, J. Erö, A. Escalante Del Valle, M. Flechl, R. Frühwirth[1], V. M. Ghete, J. Hrubec, M. Jeitler[1], N. Krammer, I. Krätschmer, D. Liko, T. Madlener, I. Mikulec, N. Rad, H. Rohringer, J. Schieck[1], R. Schöfbeck, M. Spanring, D. Spitzbart, A. Taurok, W. Waltenberger, J. Wittmann, C.-E. Wulz[1], M. Zarucki

Institute for Nuclear Problems, Minsk, Belarus
V. Chekhovsky, V. Mossolov, J. Suarez Gonzalez

Universiteit Antwerpen, Antwerpen, Belgium
E. A. De Wolf, D. Di Croce, X. Janssen, J. Lauwers, M. Pieters, H. Van Haevermaet, P. Van Mechelen, N. Van Remortel

Vrije Universiteit Brussel, Brussel, Belgium
S. Abu Zeid, F. Blekman, J. D'Hondt, J. De Clercq, K. Deroover, G. Flouris, D. Lontkovskyi, S. Lowette, I. Marchesini, S. Moortgat, L. Moreels, Q. Python, K. Skovpen, S. Tavernier, W. Van Doninck, P. Van Mulders, I. Van Parijs

Université Libre de Bruxelles, Bruxelles, Belgium
D. Beghin, B. Bilin, H. Brun, B. Clerbaux, G. De Lentdecker, H. Delannoy, B. Dorney, G. Fasanella, L. Favart, R. Goldouzian, A. Grebenyuk, A. K. Kalsi, T. Lenzi, J. Luetic, N. Postiau, E. Starling, L. Thomas, C. Vander Velde, P. Vanlaer, D. Vannerom, Q. Wang

Ghent University, Ghent, Belgium
T. Cornelis, D. Dobur, A. Fagot, M. Gul, I. Khvastunov[2], D. Poyraz, C. Roskas, D. Trocino, M. Tytgat, W. Verbeke, B. Vermassen, M. Vit, N. Zaganidis

Université Catholique de Louvain, Louvain-la-Neuve, Belgium
H. Bakhshiansohi, O. Bondu, S. Brochet, G. Bruno, C. Caputo, P. David, C. Delaere, M. Delcourt, A. Giammanco, G. Krintiras, V. Lemaitre, A. Magitteri, A. Mertens, K. Piotrzkowski, A. Saggio, M. Vidal Marono, S. Wertz, J. Zobec

Centro Brasileiro de Pesquisas Fisicas, Rio de Janeiro, Brazil
F. L. Alves, G. A. Alves, M. Correa Martins Junior, G. Correia Silva, C. Hensel, A. Moraes, M. E. Pol, P. Rebello Teles

Universidade do Estado do Rio de Janeiro, Rio de Janeiro, Brazil
E. Belchior Batista Das Chagas, W. Carvalho, J. Chinellato[3], E. Coelho, E. M. Da Costa, G. G. Da Silveira[4], D. De Jesus Damiao, C. De Oliveira Martins, S. Fonseca De Souza, H. Malbouisson, D. Matos Figueiredo, M. Melo De Almeida, C. Mora Herrera, L. Mundim, H. Nogima, W. L. Prado Da Silva, L. J. Sanchez Rosas, A. Santoro, A. Sznajder, M. Thiel, E. J. Tonelli Manganote[3], F. Torres Da Silva De Araujo, A. Vilela Pereira

Universidade Estadual Paulista[a], Universidade Federal do ABC[b], São Paulo, Brazil
S. Ahuja[a], C. A. Bernardes[a], L. Calligaris[a], T. R. Fernandez Perez Tomei[a], E. M. Gregores[b], P. G. Mercadante[b], S. F. Novaes[a], SandraS. Padula[a]

Institute for Nuclear Research and Nuclear Energy, Bulgarian Academy of Sciences, Sofia, Bulgaria
A. Aleksandrov, R. Hadjiiska, P. Iaydjiev, A. Marinov, M. Misheva, M. Rodozov, M. Shopova, G. Sultanov

University of Sofia, Sofia, Bulgaria
A. Dimitrov, L. Litov, B. Pavlov, P. Petkov

Beihang University, Beijing, China
W. Fang[5], X. Gao[5], L. Yuan

Institute of High Energy Physics, Beijing, China
M. Ahmad, J. G. Bian, G. M. Chen, H. S. Chen, M. Chen, Y. Chen, C. H. Jiang, D. Leggat, H. Liao, Z. Liu, F. Romeo, S. M. Shaheen[6], A. Spiezia, J. Tao, Z. Wang, E. Yazgan, H. Zhang, S. Zhang[6], J. Zhao

State Key Laboratory of Nuclear Physics and Technology, Peking University, Beijing, China
Y. Ban, G. Chen, A. Levin, J. Li, L. Li, Q. Li, Y. Mao, S. J. Qian, D. Wang

Tsinghua University, Beijing, China
Y. Wang

Universidad de Los Andes, Bogota, Colombia
C. Avila, A. Cabrera, C. A. Carrillo Montoya, L. F. Chaparro Sierra, C. Florez, C. F. González Hernández, M. A. Segura Delgado

University of Split, Faculty of Electrical Engineering, Mechanical Engineering and Naval Architecture, Split, Croatia
B. Courbon, N. Godinovic, D. Lelas, I. Puljak, T. Sculac

University of Split, Faculty of Science, Split, Croatia
Z. Antunovic, M. Kovac

Institute Rudjer Boskovic, Zagreb, Croatia
V. Brigljevic, D. Ferencek, K. Kadija, B. Mesic, A. Starodumov[7], T. Susa

University of Cyprus, Nicosia, Cyprus
M. W. Ather, A. Attikis, M. Kolosova, G. Mavromanolakis, J. Mousa, C. Nicolaou, F. Ptochos, P. A. Razis, H. Rykaczewski

Charles University, Prague, Czech Republic
M. Finger[8], M. Finger Jr.[8]

Escuela Politecnica Nacional, Quito, Ecuador
E. Ayala

Universidad San Francisco de Quito, Quito, Ecuador
E. Carrera Jarrin

Academy of Scientific Research and Technology of the Arab Republic of Egypt, Egyptian Network of High Energy Physics, Cairo, Egypt
Y. Assran[9,10], S. Elgammal[10], S. Khalil[11]

National Institute of Chemical Physics and Biophysics, Tallinn, Estonia
S. Bhowmik, A. Carvalho Antunes De Oliveira, R. K. Dewanjee, K. Ehataht, M. Kadastik, M. Raidal, C. Veelken

Department of Physics, University of Helsinki, Helsinki, Finland
P. Eerola, H. Kirschenmann, J. Pekkanen, M. Voutilainen

Helsinki Institute of Physics, Helsinki, Finland
J. Havukainen, J. K. Heikkilä, T. Järvinen, V. Karimäki, R. Kinnunen, T. Lampén, K. Lassila-Perini, S. Laurila, S. Lehti, T. Lindén, P. Luukka, T. Mäenpää, H. Siikonen, E. Tuominen, J. Tuominiemi

Lappeenranta University of Technology, Lappeenranta, Finland
T. Tuuva

IRFU, CEA, Université Paris-Saclay, Gif-sur-Yvette, France
M. Besancon, F. Couderc, M. Dejardin, D. Denegri, J. L. Faure, F. Ferri, S. Ganjour, A. Givernaud, P. Gras, G. Hamel de Monchenault, P. Jarry, C. Leloup, E. Locci, J. Malcles, G. Negro, J. Rander, A. Rosowsky, M. Ö. Sahin, M. Titov

Laboratoire Leprince-Ringuet, Ecole polytechnique, CNRS/IN2P3, Université Paris-Saclay, Palaiseau, France
A. Abdulsalam[12], C. Amendola, I. Antropov, F. Beaudette, P. Busson, C. Charlot, R. Granier de Cassagnac, I. Kucher, A. Lobanov, J. Martin Blanco, C. Martin Perez, M. Nguyen, C. Ochando, G. Ortona, P. Paganini, P. Pigard, J. Rembser, R. Salerno, J. B. Sauvan, Y. Sirois, A. G. Stahl Leiton, A. Zabi, A. Zghiche

Université de Strasbourg, CNRS, IPHC UMR 7178, Strasbourg, France
J.-L. Agram[13], J. Andrea, D. Bloch, J.-M. Brom, E. C. Chabert, V Cherepanov, C. Collard, E. Conte[13], J.-C. Fontaine[13], D. Gelé, U. Goerlach, M. Jansová, A.-C. Le Bihan, N. Tonon, P. Van Hove

Centre de Calcul de l'Institut National de Physique Nucleaire et de Physique des Particules, CNRS/IN2P3, Villeurbanne, France
S. Gadrat

Université de Lyon, Université Claude Bernard Lyon 1, CNRS-IN2P3, Institut de Physique Nucléaire de Lyon, Villeurbanne, France
S. Beauceron, C. Bernet, G. Boudoul, N. Chanon, R. Chierici, D. Contardo, P. Depasse, H. El Mamouni, J. Fay, L. Finco, S. Gascon, M. Gouzevitch, G. Grenier, B. Ille, F. Lagarde, I. B. Laktineh, H. Lattaud, M. Lethuillier, L. Mirabito, S. Perries, A. Popov[14], V. Sordini, G. Touquet, M. Vander Donckt, S. Viret

Georgian Technical University, Tbilisi, Georgia
A. Khvedelidze[8]

Tbilisi State University, Tbilisi, Georgia
Z. Tsamalaidze[8]

RWTH Aachen University, I. Physikalisches Institut, Aachen, Germany
C. Autermann, L. Feld, M. K. Kiesel, K. Klein, M. Lipinski, M. Preuten, M. P. Rauch, C. Schomakers, J. Schulz, M. Teroerde, B. Wittmer

RWTH Aachen University, III. Physikalisches Institut A, Aachen, Germany
A. Albert, D. Duchardt, M. Erdmann, S. Erdweg, T. Esch, R. Fischer, S. Ghosh, A. Güth, T. Hebbeker, C. Heidemann, K. Hoepfner, H. Keller, L. Mastrolorenzo, M. Merschmeyer, A. Meyer, P. Millet, S. Mukherjee, T. Pook, M. Radziej, H. Reithler, M. Rieger, A. Schmidt, D. Teyssier, S. Thüer

RWTH Aachen University, III. Physikalisches Institut B, Aachen, Germany
G. Flügge, O. Hlushchenko, T. Kress, A. Künsken, T. Müller, A. Nehrkorn, A. Nowack, C. Pistone, O. Pooth, D. Roy, H. Sert, A. Stahl[15]

Deutsches Elektronen-Synchrotron, Hamburg, Germany
M. Aldaya Martin, T. Arndt, C. Asawatangtrakuldee, I. Babounikau, K. Beernaert, O. Behnke, U. Behrens, A. Bermúdez Martínez, D. Bertsche, A. A. Bin Anuar, K. Borras[16], V. Botta, A. Campbell, P. Connor, C. Contreras-Campana, V. Danilov, A. De Wit, M. M. Defranchis, C. Diez Pardos, D. Domínguez Damiani, G. Eckerlin, T. Eichhorn, A. Elwood, E. Eren, E. Gallo[17], A. Geiser, J. M. Grados Luyando, A. Grohsjean, M. Guthoff, M. Haranko, A. Harb, J. Hauk, H. Jung, M. Kasemann, J. Keaveney, C. Kleinwort, J. Knolle, D. Krücker, W. Lange, A. Lelek, T. Lenz, J. Leonard, K. Lipka, W. Lohmann[18], R. Mankel, I.-A. Melzer-Pellmann, A. B. Meyer, M. Meyer, M. Missiroli, G. Mittag, J. Mnich, V. Myronenko, S. K. Pflitsch, D. Pitzl, A. Raspereza, M. Savitskyi, P. Saxena, P. Schütze, C. Schwanenberger, R. Shevchenko, A. Singh, H. Tholen, O. Turkot, A. Vagnerini, G. P. Van Onsem, R. Walsh, Y. Wen, K. Wichmann, C. Wissing, O. Zenaiev

University of Hamburg, Hamburg, Germany
R. Aggleton, S. Bein, L. Benato, A. Benecke, V. Blobel, T. Dreyer, A. Ebrahimi, E. Garutti, D. Gonzalez, P. Gunnellini, J. Haller, A. Hinzmann, A. Karavdina, G. Kasieczka, R. Klanner, R. Kogler, N. Kovalchuk, S. Kurz, V. Kutzner, J. Lange, D. Marconi, J. Multhaup, M. Niedziela, C.E.N. Niemeyer, D. Nowatschin, A. Perieanu, A. Reimers, O. Rieger, C. Scharf, P. Schleper, S. Schumann, J. Schwandt, J. Sonneveld, H. Stadie, G. Steinbrück, F. M. Stober, M. Stöver, A. Vanhoefer, B. Vormwald, I. Zoi

Karlsruher Institut fuer Technologie, Karlsruhe, Germany
M. Akbiyik, C. Barth, M. Baselga, S. Baur, E. Butz, R. Caspart, T. Chwalek, F. Colombo, W. De Boer, A. Dierlamm, K. El Morabit, N. Faltermann, B. Freund, M. Giffels, M. A. Harrendorf, F. Hartmann[15], S. M. Heindl, U. Husemann, I. Katkov[14], S. Kudella, S. Mitra, M. U. Mozer, Th. Müller, M. Musich, M. Plagge, G. Quast, K. Rabbertz, M. Schröder, I. Shvetsov, H. J. Simonis, R. Ulrich, S. Wayand, M. Weber, T. Weiler, C. Wöhrmann, R. Wolf

Institute of Nuclear and Particle Physics (INPP), NCSR Demokritos, Aghia Paraskevi, Greece
G. Anagnostou, G. Daskalakis, T. Geralis, A. Kyriakis, D. Loukas, G. Paspalaki, I. Topsis-Giotis

National and Kapodistrian University of Athens, Athens, Greece
G. Karathanasis, S. Kesisoglou, P. Kontaxakis, A. Panagiotou, I. Papavergou, N. Saoulidou, E. Tziaferi, K. Vellidis

National Technical University of Athens, Athens, Greece
K. Kousouris, I. Papakrivopoulos, G. Tsipolitis

University of Ioánnina, Ioánnina, Greece
I. Evangelou, C. Foudas, P. Gianneios, P. Katsoulis, P. Kokkas, S. Mallios, N. Manthos, I. Papadopoulos, E. Paradas, J. Strologas, F. A. Triantis, D. Tsitsonis

MTA-ELTE Lendület CMS Particle and Nuclear Physics Group, Eötvös Loránd University, Budapest, Hungary
M. Bartók[19], M. Csanad, N. Filipovic, P. Major, M. I. Nagy, G. Pasztor, O. Surányi, G. I. Veres

Wigner Research Centre for Physics, Budapest, Hungary
G. Bencze, C. Hajdu, D. Horvath[20], Á. Hunyadi, F. Sikler, T. Á. Vámi, V. Veszpremi, G. Vesztergombi[†]

Institute of Nuclear Research ATOMKI, Debrecen, Hungary
N. Beni, S. Czellar, J. Karancsi[21], A. Makovec, J. Molnar, Z. Szillasi

Institute of Physics, University of Debrecen, Debrecen, Hungary
P. Raics, Z. L. Trocsanyi, B. Ujvari

Indian Institute of Science (IISc), Bangalore, India
S. Choudhury, J. R. Komaragiri, P. C. Tiwari

National Institute of Science Education and Research, HBNI, Bhubaneswar, India
S. Bahinipati[22], C. Kar, P. Mal, K. Mandal, A. Nayak[23], D. K. Sahoo[22], S. K. Swain

Panjab University, Chandigarh, India
S. Bansal, S. B. Beri, V. Bhatnagar, S. Chauhan, R. Chawla, N. Dhingra, R. Gupta, A. Kaur, M. Kaur, S. Kaur, P. Kumari, M. Lohan, A. Mehta, K. Sandeep, S. Sharma, J. B. Singh, A. K. Virdi, G. Walia

University of Delhi, Delhi, India
A. Bhardwaj, B. C. Choudhary, R. B. Garg, M. Gola, S. Keshri, Ashok Kumar, S. Malhotra, M. Naimuddin, P. Priyanka, K. Ranjan, Aashaq Shah, R. Sharma

Saha Institute of Nuclear Physics, HBNI, Kolkata, India
R. Bhardwaj[24], M. Bharti[24], R. Bhattacharya, S. Bhattacharya, U. Bhawandeep[24], D. Bhowmik, S. Dey, S. Dutt[24], S. Dutta, S. Ghosh, K. Mondal, S. Nandan, A. Purohit, P. K. Rout, A. Roy, S. Roy Chowdhury, G. Saha, S. Sarkar, M. Sharan, B. Singh[24], S. Thakur[24]

Indian Institute of Technology Madras, Madras, India
P. K. Behera

Bhabha Atomic Research Centre, Mumbai, India
R. Chudasama, D. Dutta, V. Jha, V. Kumar, P. K. Netrakanti, L. M. Pant, P. Shukla

Tata Institute of Fundamental Research-A, Mumbai, India
T. Aziz, M. A. Bhat, S. Dugad, G. B. Mohanty, N. Sur, B. Sutar, RavindraKumar Verma

Tata Institute of Fundamental Research-B, Mumbai, India
S. Banerjee, S. Bhattacharya, S. Chatterjee, P. Das, M. Guchait, Sa. Jain, S. Karmakar, S. Kumar, M. Maity[25], G. Majumder, K. Mazumdar, N. Sahoo, T. Sarkar[25]

Indian Institute of Science Education and Research (IISER), Pune, India
S. Chauhan, S. Dube, V. Hegde, A. Kapoor, K. Kothekar, S. Pandey, A. Rane, S. Sharma

Institute for Research in Fundamental Sciences (IPM), Tehran, Iran
S. Chenarani[26], E. Eskandari Tadavani, S. M. Etesami[26], M. Khakzad, M. Mohammadi Najafabadi, M. Naseri, F. Rezaei Hosseinabadi, B. Safarzadeh[27], M. Zeinali

University College Dublin, Dublin, Ireland
M. Felcini, M. Grunewald

INFN Sezione di Bari[a], Università di Bari[b], Politecnico di Bari[c], Bari, Italy
M. Abbrescia[a,b], C. Calabria[a,b], A. Colaleo[a], D. Creanza[a,c], L. Cristella[a,b], N. De Filippis[a,c], M. De Palma[a,b], A. Di Florio[a,b], F. Errico[a,b], L. Fiore[a], A. Gelmi[a,b], G. Iaselli[a,c], M. Ince[a,b], S. Lezki[a,b], G. Maggi[a,c], M. Maggi[a], G. Miniello[a,b], S. My[a,b], S. Nuzzo[a,b], A. Pompili[a,b], G. Pugliese[a,c], R. Radogna[a], A. Ranieri[a], G. Selvaggi[a,b], A. Sharma[a], L. Silvestris[a], R. Venditti[a], P. Verwilligen[a], G. Zito[a]

INFN Sezione di Bologna[a], Università di Bologna[b], Bologna, Italy
G. Abbiendi[a], C. Battilana[a,b], D. Bonacorsi[a,b], L. Borgonovi[a,b], S. Braibant-Giacomelli[a,b], R. Campanini[a,b], P. Capiluppi[a,b], A. Castro[a,b], F. R. Cavallo[a], S. S. Chhibra[a,b], C. Ciocca[a], G. Codispoti[a,b], M. Cuffiani[a,b], G. M. Dallavalle[a], F. Fabbri[a], A. Fanfani[a,b], E. Fontanesi, P. Giacomelli[a], C. Grandi[a], L. Guiducci[a,b], S. Lo Meo[a], S. Marcellini[a], G. Masetti[a], A. Montanari[a], F. L. Navarria[a,b], A. Perrotta[a], F. Primavera[a,b,15], A. M. Rossi[a,b], T. Rovelli[a,b], G. P. Siroli[a,b], N. Tosi[a]

INFN Sezione di Catania[a], Università di Catania[b], Catania, Italy
S. Albergo[a,b], A. Di Mattia[a], R. Potenza[a,b], A. Tricomi[a,b], C. Tuve[a,b]

INFN Sezione di Firenze[a], Università di Firenze[b], Firenze, Italy
G. Barbagli[a], K. Chatterjee[a,b], V. Ciulli[a,b], C. Civinini[a], R. D'Alessandro[a,b], E. Focardi[a,b], G. Latino, P. Lenzi[a,b], M. Meschini[a], S. Paoletti[a], L. Russo[a,28], G. Sguazzoni[a], D. Strom[a], L. Viliani[a]

INFN Laboratori Nazionali di Frascati, Frascati, Italy
L. Benussi, S. Bianco, F. Fabbri, D. Piccolo

INFN Sezione di Genova[a], Università di Genova[b], Genova, Italy
F. Ferro[a], R. Mulargia[a,b], F. Ravera[a,b], E. Robutti[a], S. Tosi[a,b]

INFN Sezione di Milano-Bicocca[a], Università di Milano-Bicocca[b], Milano, Italy
A. Benaglia[a], A. Beschi[b], F. Brivio[a,b], V. Ciriolo[a,b,15], S. Di Guida[a,d,15], M. E. Dinardo[a,b], S. Fiorendi[a,b], S. Gennai[a], A. Ghezzi[a,b], P. Govoni[a,b], M. Malberti[a,b], S. Malvezzi[a], A. Massironi[a,b], D. Menasce[a], F. Monti, L. Moroni[a], M. Paganoni[a,b], D. Pedrini[a], S. Ragazzi[a,b], T. Tabarelli de Fatis[a,b], D. Zuolo[a,b]

INFN Sezione di Napoli[a], Università di Napoli 'Federico II' [b], Napoli, Italy, Università della Basilicata[c], Potenza, Italy, Università G. Marconi[d], Roma, Italy
S. Buontempo[a], N. Cavallo[a,c], A. De Iorio[a,b], F. Fabozzi[a,c], F. Fienga[a], G. Galati[a], A. O. M. Iorio[a,b], W. A. Khan[a], L. Lista[a], S. Meola[a,d,15], P. Paolucci[a,15], C. Sciacca[a,b], E. Voevodina[a,b]

INFN Sezione di Padova[a], Università di Padova[b], Padova, Italy, Università di Trento[c], Trento, Italy
P. Azzi[a], N. Bacchetta[a], D. Bisello[a,b], A. Boletti[a,b], A. Bragagnolo, R. Carlin[a,b], P. Checchia[a], M. Dall'Osso[a,b], P. De Castro Manzano[a], T. Dorigo[a], U. Gasparini[a,b], A. Gozzelino[a], S. Y. Hoh, S. Lacaprara[a], P. Lujan, M. Margoni[a,b], A. T. Meneguzzo[a,b], M. Passaseo[a], J. Pazzini[a], N. Pozzobon[a,b], P. Ronchese[a,b], R. Rossin[a,b], F. Simonetto[a,b], A. Tiko, E. Torassa[a], M. Tosi[a,b], M. Zanetti[a,b], P. Zotto[a,b], G. Zumerle[a,b]

INFN Sezione di Pavia[a], Università di Pavia[b], Pavia, Italy
A. Braghieri[a], A. Magnani[a], P. Montagna[a,b], S. P. Ratti[a,b], V. Re[a], M. Ressegotti[a,b], C. Riccardi[a,b], P. Salvini[a], I. Vai[a,b], P. Vitulo[a,b]

INFN Sezione di Perugia[a], Università di Perugia[b], Perugia, Italy
M. Biasini[a,b], G. M. Bilei[a], C. Cecchi[a,b], D. Ciangottini[a,b], L. Fanò[a,b], P. Lariccia[a,b], R. Leonardi[a,b], E. Manoni[a], G. Mantovani[a,b], V. Mariani[a,b], M. Menichelli[a], A. Rossi[a,b], A. Santocchia[a,b], D. Spiga[a]

INFN Sezione di Pisa[a], Università di Pisa[b], Scuola Normale Superiore di Pisa[c], Pisa, Italy
K. Androsov[a], P. Azzurri[a], G. Bagliesi[a], L. Bianchini[a], T. Boccali[a], L. Borrello, R. Castaldi[a], M. A. Ciocci[a,b], R. Dell'Orso[a], G. Fedi[a], F. Fiori[a,c], L. Giannini[a,c], A. Giassi[a], M. T. Grippo[a], F. Ligabue[a,c], E. Manca[a,c], G. Mandorli[a,c], A. Messineo[a,b], F. Palla[a], A. Rizzi[a,b], G. Rolandi[29], P. Spagnolo[a], R. Tenchini[a], G. Tonelli[a,b], A. Venturi[a], P. G. Verdini[a]

INFN Sezione di Roma[a], Sapienza Università di Roma[b], Rome, Italy
L. Barone[a,b], F. Cavallari[a], M. Cipriani[a,b], D. Del Re[a,b], E. Di Marco[a,b], M. Diemoz[a], S. Gelli[a,b], E. Longo[a,b], B. Marzocchi[a,b], P. Meridiani[a], G. Organtini[a,b], F. Pandolfi[a], R. Paramatti[a,b], F. Preiato[a,b], S. Rahatlou[a,b], C. Rovelli[a], F. Santanastasio[a,b]

INFN Sezione di Torino[a], Università di Torino[b], Torino, Italy, Università del Piemonte Orientale[c], Novara, Italy
N. Amapane[a,b], R. Arcidiacono[a,c], S. Argiro[a,b], M. Arneodo[a,c], N. Bartosik[a], R. Bellan[a,b], C. Biino[a], N. Cartiglia[a], F. Cenna[a,b], S. Cometti[a], M. Costa[a,b], R. Covarelli[a,b], N. Demaria[a], B. Kiani[a,b], C. Mariotti[a], S. Maselli[a], E. Migliore[a,b], V. Monaco[a,b], E. Monteil[a,b], M. Monteno[a], M. M. Obertino[a,b], L. Pacher[a,b], N. Pastrone[a], M. Pelliccioni[a], G. L. Pinna Angioni[a,b], A. Romero[a,b], M. Ruspa[a,c], R. Sacchi[a,b], K. Shchelina[a,b], V. Sola[a], A. Solano[a,b], D. Soldi[a,b], A. Staiano[a]

INFN Sezione di Trieste[a], Università di Trieste[b], Trieste, Italy
S. Belforte[a], V. Candelise[a,b], M. Casarsa[a], F. Cossutti[a], A. Da Rold[a,b], G. Della Ricca[a,b], F. Vazzoler[a,b], A. Zanetti[a]

Kyungpook National University, Daegu, Korea
D. H. Kim, G. N. Kim, M. S. Kim, J. Lee, S. Lee, S. W. Lee, C. S. Moon, Y. D. Oh, S. I. Pak, S. Sekmen, D. C. Son, Y. C. Yang

Chonnam National University, Institute for Universe and Elementary Particles, Kwangju, Korea
H. Kim, D. H. Moon, G. Oh

Hanyang University, Seoul, Korea
B. Francois, J. Goh[30], T. J. Kim

Korea University, Seoul, Korea
S. Cho, S. Choi, Y. Go, D. Gyun, S. Ha, B. Hong, Y. Jo, K. Lee, K. S. Lee, S. Lee, J. Lim, S. K. Park, Y. Roh

Sejong University, Seoul, Korea
H. S. Kim

Seoul National University, Seoul, Korea
J. Almond, J. Kim, J. S. Kim, H. Lee, K. Lee, K. Nam, S. B. Oh, B. C. Radburn-Smith, S. h. Seo, U. K. Yang, H. D. Yoo, G. B. Yu

University of Seoul, Seoul, Korea
D. Jeon, H. Kim, J. H. Kim, J. S. H. Lee, I. C. Park

Sungkyunkwan University, Suwon, Korea
Y. Choi, C. Hwang, J. Lee, I. Yu

Vilnius University, Vilnius, Lithuania
V. Dudenas, A. Juodagalvis, J. Vaitkus

National Centre for Particle Physics, Universiti Malaya, Kuala Lumpur, Malaysia
I. Ahmed, Z. A. Ibrahim, M. A. B. Md Ali[31], F. Mohamad Idris[32], W. A. T. Wan Abdullah, M. N. Yusli, Z. Zolkapli

Universidad de Sonora (UNISON), Hermosillo, Mexico
J. F. Benitez, A. Castaneda Hernandez, J. A. Murillo Quijada

Centro de Investigacion y de Estudios Avanzados del IPN, Mexico City, Mexico
H. Castilla-Valdez, E. De La Cruz-Burelo, M. C. Duran-Osuna, I. Heredia-De La Cruz[33], R. Lopez-Fernandez, J. Mejia Guisao, R. I. Rabadan-Trejo, M. Ramirez-Garcia, G. Ramirez-Sanchez, R Reyes-Almanza, A. Sanchez-Hernandez

Universidad Iberoamericana, Mexico City, Mexico
S. Carrillo Moreno, C. Oropeza Barrera, F. Vazquez Valencia

Benemerita Universidad Autonoma de Puebla, Puebla, Mexico
J. Eysermans, I. Pedraza, H. A. Salazar Ibarguen, C. Uribe Estrada

Universidad Autónoma de San Luis Potosí, San Luis Potosí, Mexico
A. Morelos Pineda

University of Auckland, Auckland, New Zealand
D. Krofcheck

University of Canterbury, Christchurch, New Zealand
S. Bheesette, P. H. Butler

National Centre for Physics, Quaid-I-Azam University, Islamabad, Pakistan
A. Ahmad, M. Ahmad, M. I. Asghar, Q. Hassan, H. R. Hoorani, A. Saddique, M. A. Shah, M. Shoaib, M. Waqas

National Centre for Nuclear Research, Swierk, Poland
H. Bialkowska, M. Bluj, B. Boimska, T. Frueboes, M. Górski, M. Kazana, M. Szleper, P. Traczyk, P. Zalewski

Institute of Experimental Physics, Faculty of Physics, University of Warsaw, Warsaw, Poland
K. Bunkowski, A. Byszuk[34], K. Doroba, A. Kalinowski, M. Konecki, J. Krolikowski, M. Misiura, M. Olszewski, A. Pyskir, M. Walczak

Laboratório de Instrumentação e Física Experimental de Partículas, Lisboa, Portugal
M. Araujo, P. Bargassa, C. Beirão Da Cruz E Silva, A. Di Francesco, P. Faccioli, B. Galinhas, M. Gallinaro, J. Hollar, N. Leonardo, J. Seixas, G. Strong, O. Toldaiev, J. Varela

Joint Institute for Nuclear Research, Dubna, Russia
S. Afanasiev, P. Bunin, M. Gavrilenko, I. Golutvin, I. Gorbunov, A. Kamenev, V. Karjavine, A. Lanev, A. Malakhov, V. Matveev[35,36], P. Moisenz, V. Palichik, V. Perelygin, S. Shmatov, S. Shulha, N. Skatchkov, V. Smirnov, N. Voytishin, A. Zarubin

Petersburg Nuclear Physics Institute, Gatchina (St. Petersburg), Russia
V. Golovtsov, Y. Ivanov, V. Kim[37], E. Kuznetsova[38], P. Levchenko, V. Murzin, V. Oreshkin, I. Smirnov, D. Sosnov, V. Sulimov, L. Uvarov, S. Vavilov, A. Vorobyev

Institute for Nuclear Research, Moscow, Russia
Yu. Andreev, A. Dermenev, S. Gninenko, N. Golubev, A. Karneyeu, M. Kirsanov, N. Krasnikov, A. Pashenkov, D. Tlisov, A. Toropin

Institute for Theoretical and Experimental Physics, Moscow, Russia
V. Epshteyn, V. Gavrilov, N. Lychkovskaya, V. Popov, I. Pozdnyakov, G. Safronov, A. Spiridonov, A. Stepennov, V. Stolin, M. Toms, E. Vlasov, A. Zhokin

Moscow Institute of Physics and Technology, Moscow, Russia
T. Aushev

National Research Nuclear University 'Moscow Engineering Physics Institute' (MEPhI), Moscow, Russia
R. Chistov[39], M. Danilov[39], P. Parygin, D. Philippov, S. Polikarpov[39], E. Tarkovskii

P.N. Lebedev Physical Institute, Moscow, Russia
V. Andreev, M. Azarkin, I. Dremin[36], M. Kirakosyan, A. Terkulov

Skobeltsyn Institute of Nuclear Physics, Lomonosov Moscow State University, Moscow, Russia
A. Baskakov, A. Belyaev, E. Boos, V. Bunichev, M. Dubinin[40], L. Dudko, A. Gribushin, V. Klyukhin, O. Kodolova, I. Lokhtin, I. Miagkov, S. Obraztsov, S. Petrushanko, V. Savrin, A. Snigirev

Novosibirsk State University (NSU), Novosibirsk, Russia
A. Barnyakov[41], V. Blinov[41], T. Dimova[41], L. Kardapoltsev[41], Y. Skovpen[41]

Institute for High Energy Physics of National Research Centre 'Kurchatov Institute', Protvino, Russia
I. Azhgirey, I. Bayshev, S. Bitioukov, D. Elumakhov, A. Godizov, V. Kachanov, A. Kalinin, D. Konstantinov, P. Mandrik, V. Petrov, R. Ryutin, S. Slabospitskii, A. Sobol, S. Troshin, N. Tyurin, A. Uzunian, A. Volkov

National Research Tomsk Polytechnic University, Tomsk, Russia
A. Babaev, S. Baidali, V. Okhotnikov

University of Belgrade, Faculty of Physics and Vinca Institute of Nuclear Sciences, Belgrade, Serbia
P. Adzic[42], P. Cirkovic, D. Devetak, M. Dordevic, J. Milosevic

Centro de Investigaciones Energéticas Medioambientales y Tecnológicas (CIEMAT), Madrid, Spain
J. Alcaraz Maestre, A. Álvarez Fernández, I. Bachiller, M. Barrio Luna, J. A. Brochero Cifuentes, M. Cerrada, N. Colino, B. De La Cruz, A. Delgado Peris, C. Fernandez Bedoya, J. P. Fernández Ramos, J. Flix, M. C. Fouz, O. Gonzalez Lopez, S. Goy Lopez, J. M. Hernandez, M. I. Josa, D. Moran, A. Pérez-Calero Yzquierdo, J. Puerta Pelayo, I. Redondo, L. Romero, M. S. Soares, A. Triossi

Universidad Autónoma de Madrid, Madrid, Spain
C. Albajar, J. F. de Trocóniz

Universidad de Oviedo, Oviedo, Spain
J. Cuevas, C. Erice, J. Fernandez Menendez, S. Folgueras, I. Gonzalez Caballero, J. R. González Fernández, E. Palencia Cortezon, V. Rodríguez Bouza, S. Sanchez Cruz, P. Vischia, J. M. Vizan Garcia

Instituto de Física de Cantabria (IFCA), CSIC-Universidad de Cantabria, Santander, Spain
I. J. Cabrillo, A. Calderon, B. Chazin Quero, J. Duarte Campderros, M. Fernandez, P. J. Fernández Manteca, A. García Alonso, J. Garcia-Ferrero, G. Gomez, A. Lopez Virto, J. Marco, C. Martinez Rivero, P. Martinez Ruiz del Arbol, F. Matorras, J. Piedra Gomez, C. Prieels, T. Rodrigo, A. Ruiz-Jimeno, L. Scodellaro, N. Trevisani, I. Vila, R. Vilar Cortabitarte

Department of Physics, University of Ruhuna, Matara, Sri Lanka
N. Wickramage

CERN, European Organization for Nuclear Research, Geneva, Switzerland
D. Abbaneo, B. Akgun, E. Auffray, G. Auzinger, P. Baillon, A. H. Ball, D. Barney, J. Bendavid, M. Bianco, A. Bocci, C. Botta, E. Brondolin, T. Camporesi, M. Cepeda, G. Cerminara, E. Chapon, Y. Chen, G. Cucciati, D. d'Enterria, A. Dabrowski, N. Daci, V. Daponte, A. David, A. De Roeck, N. Deelen, M. Dobson, M. Dünser, N. Dupont, A. Elliott-Peisert, P. Everaerts, F. Fallavollita[43], D. Fasanella, G. Franzoni, J. Fulcher, W. Funk, D. Gigi, A. Gilbert, K. Gill, F. Glege, M. Gruchala, M. Guilbaud, D. Gulhan, J. Hegeman, C. Heidegger, V. Innocente, A. Jafari, P. Janot, O. Karacheban[18], J. Kieseler, A. Kornmayer, M. Krammer[1], C. Lange, P. Lecoq, C. Lourenço, L. Malgeri, M. Mannelli, F. Meijers, J. A. Merlin, S. Mersi, E. Meschi, P. Milenovic[44], F. Moortgat, M. Mulders, J. Ngadiuba, S. Nourbakhsh, S. Orfanelli, L. Orsini, F. Pantaleo[15], L. Pape, E. Perez, M. Peruzzi, A. Petrilli, G. Petrucciani, A. Pfeiffer, M. Pierini, F. M. Pitters, D. Rabady, A. Racz, T. Reis, M. Rovere, H. Sakulin, C. Schäfer, C. Schwick, M. Seidel, M. Selvaggi, A. Sharma, P. Silva, P. Sphicas[45], A. Stakia, J. Steggemann, D. Treille, A. Tsirou, V. Veckalns[46], M. Verzetti, W. D. Zeuner

Paul Scherrer Institut, Villigen, Switzerland
L. Caminada[47], K. Deiters, W. Erdmann, R. Horisberger, Q. Ingram, H. C. Kaestli, D. Kotlinski, U. Langenegger, T. Rohe, S. A. Wiederkehr

Institute for Particle Physics and Astrophysics (IPA), ETH Zurich, Zurich, Switzerland
M. Backhaus, L. Bäni, P. Berger, N. Chernyavskaya, G. Dissertori, M. Dittmar, M. Donegà, C. Dorfer, T. A. Gómez Espinosa, C. Grab, D. Hits, T. Klijnsma, W. Lustermann, R. A. Manzoni, M. Marionneau, M. T. Meinhard, F. Micheli, P. Musella, F. Nessi-Tedaldi, J. Pata, F. Pauss, G. Perrin, L. Perrozzi, S. Pigazzini, M. Quittnat, C. Reissel, D. Ruini, D. A. Sanz Becerra, M. Schönenberger, L. Shchutska, V. R. Tavolaro, K. Theofilatos, M. L. Vesterbacka Olsson, R. Wallny, D. H. Zhu

Universität Zürich, Zurich, Switzerland
T. K. Aarrestad, C. Amsler[48], D. Brzhechko, M. F. Canelli, A. De Cosa, R. Del Burgo, S. Donato, C. Galloni, T. Hreus, B. Kilminster, S. Leontsinis, I. Neutelings, G. Rauco, P. Robmann, D. Salerno, K. Schweiger, C. Seitz, Y. Takahashi, A. Zucchetta

National Central University, Chung-Li, Taiwan
Y. H. Chang, K. y. Cheng, T. H. Doan, R. Khurana, C. M. Kuo, W. Lin, A. Pozdnyakov, S. S. Yu

National Taiwan University (NTU), Taipei, Taiwan
P. Chang, Y. Chao, K. F. Chen, P. H. Chen, W.-S. Hou, Arun Kumar, Y. F. Liu, R.-S. Lu, E. Paganis, A. Psallidas, A. Steen

Chulalongkorn University, Faculty of Science, Department of Physics, Bangkok, Thailand
B. Asavapibhop, N. Srimanobhas, N. Suwonjandee

Çukurova University, Physics Department, Science and Art Faculty, Adana, Turkey
A. Bat, F. Boran, S. Cerci[49], S. Damarseckin, Z. S. Demiroglu, F. Dolek, C. Dozen, I. Dumanoglu, S. Girgis, G. Gokbulut, Y. Guler, E. Gurpinar, I. Hos[50], C. Isik, E. E. Kangal[51], O. Kara, A. Kayis Topaksu, U. Kiminsu, M. Oglakci, G. Onengut, K. Ozdemir[52], S. Ozturk[53], B. Tali[49], U. G. Tok, H. Topakli[53], S. Turkcapar, I. S. Zorbakir, C. Zorbilmez

Middle East Technical University, Physics Department, Ankara, Turkey
B. Isildak[54], G. Karapinar[55], M. Yalvac, M. Zeyrek

Bogazici University, Istanbul, Turkey
I. O. Atakisi, E. Gülmez, M. Kaya[56], O. Kaya[57], S. Ozkorucuklu[58], S. Tekten, E. A. Yetkin[59]

Istanbul Technical University, Istanbul, Turkey
M. N. Agaras, A. Cakir, K. Cankocak, Y. Komurcu, S. Sen[60]

Institute for Scintillation Materials of National Academy of Science of Ukraine, Kharkov, Ukraine
B. Grynyov

National Scientific Center, Kharkov Institute of Physics and Technology, Kharkov, Ukraine
L. Levchuk

University of Bristol, Bristol, United Kingdom
F. Ball, L. Beck, J. J. Brooke, D. Burns, E. Clement, D. Cussans, O. Davignon, H. Flacher, J. Goldstein, G. P. Heath, H. F. Heath, L. Kreczko, D. M. Newbold[61], S. Paramesvaran, B. Penning, T. Sakuma, D. Smith, V. J. Smith, J. Taylor, A. Titterton

Rutherford Appleton Laboratory, Didcot, United Kingdom
K. W. Bell, A. Belyaev[62], C. Brew, R. M. Brown, D. Cieri, D. J. A. Cockerill, J. A. Coughlan, K. Harder, S. Harper, J. Linacre, E. Olaiya, D. Petyt, C. H. Shepherd-Themistocleous, A. Thea, I. R. Tomalin, T. Williams, W. J. Womersley

Imperial College, London, United Kingdom
R. Bainbridge, P. Bloch, J. Borg, S. Breeze, O. Buchmuller, A. Bundock, D. Colling, P. Dauncey, G. Davies, M. Della Negra, R. Di Maria, G. Hall, G. Iles, T. James, M. Komm, C. Laner, L. Lyons, A.-M. Magnan, S. Malik, A. Martelli, J. Nash[63], A. Nikitenko[7], V. Palladino, M. Pesaresi, D. M. Raymond, A. Richards, A. Rose, E. Scott, C. Seez, A. Shtipliyski, G. Singh, M. Stoye, T. Strebler, S. Summers, A. Tapper, K. Uchida, T. Virdee[15], N. Wardle, D. Winterbottom, J. Wright, S. C. Zenz

Brunel University, Uxbridge, United Kingdom
J. E. Cole, P. R. Hobson, A. Khan, P. Kyberd, C. K. Mackay, A. Morton, I. D. Reid, L. Teodorescu, S. Zahid

Baylor University, Waco, USA
K. Call, J. Dittmann, K. Hatakeyama, H. Liu, C. Madrid, B. McMaster, N. Pastika, C. Smith

Catholic University of America, Washington DC, USA
R. Bartek, A. Dominguez

The University of Alabama, Tuscaloosa, USA
A. Buccilli, S. I. Cooper, C. Henderson, P. Rumerio, C. West

Boston University, Boston, USA
D. Arcaro, T. Bose, D. Gastler, D. Pinna, D. Rankin, C. Richardson, J. Rohlf, L. Sulak, D. Zou

Brown University, Providence, USA
G. Benelli, X. Coubez, D. Cutts, M. Hadley, J. Hakala, U. Heintz, J. M. Hogan[64], K. H. M. Kwok, E. Laird, G. Landsberg, J. Lee, Z. Mao, M. Narain, S. Sagir[65], R. Syarif, E. Usai, D. Yu

University of California, Davis, Davis, USA
R. Band, C. Brainerd, R. Breedon, D. Burns, M. Calderon De La Barca Sanchez, M. Chertok, J. Conway, R. Conway, P. T. Cox, R. Erbacher, C. Flores, G. Funk, W. Ko, O. Kukral, R. Lander, M. Mulhearn, D. Pellett, J. Pilot, S. Shalhout, M. Shi, D. Stolp, D. Taylor, K. Tos, M. Tripathi, Z. Wang, F. Zhang

University of California, Los Angeles, USA
M. Bachtis, C. Bravo, R. Cousins, A. Dasgupta, A. Florent, J. Hauser, M. Ignatenko, N. Mccoll, S. Regnard, D. Saltzberg, C. Schnaible, V. Valuev

University of California, Riverside, Riverside, USA
E. Bouvier, K. Burt, R. Clare, J. W. Gary, S. M. A. Ghiasi Shirazi, G. Hanson, G. Karapostoli, E. Kennedy, F. Lacroix, O. R. Long, M. Olmedo Negrete, M. I. Paneva, W. Si, L. Wang, H. Wei, S. Wimpenny, B. R. Yates

University of California, San Diego, La Jolla, USA
J. G. Branson, P. Chang, S. Cittolin, M. Derdzinski, R. Gerosa, D. Gilbert, B. Hashemi, A. Holzner, D. Klein, G. Kole, V. Krutelyov, J. Letts, M. Masciovecchio, D. Olivito, S. Padhi, M. Pieri, M. Sani, V. Sharma, S. Simon, M. Tadel, A. Vartak, S. Wasserbaech[66], J. Wood, F. Würthwein, A. Yagil, G. Zevi Della Porta

Department of Physics, University of California, Santa Barbara, Santa Barbara, USA
N. Amin, R. Bhandari, J. Bradmiller-Feld, C. Campagnari, M. Citron, A. Dishaw, V. Dutta, M. Franco Sevilla, L. Gouskos, R. Heller, J. Incandela, A. Ovcharova, H. Qu, J. Richman, D. Stuart, I. Suarez, S. Wang, J. Yoo

California Institute of Technology, Pasadena, USA
D. Anderson, A. Bornheim, J. M. Lawhorn, N. Lu, H. B. Newman, T. Q. Nguyen, M. Spiropulu, J. R. Vlimant, R. Wilkinson, S. Xie, Z. Zhang, R. Y. Zhu

Carnegie Mellon University, Pittsburgh, USA
M. B. Andrews, T. Ferguson, T. Mudholkar, M. Paulini, M. Sun, I. Vorobiev, M. Weinberg

University of Colorado Boulder, Boulder, USA
J. P. Cumalat, W. T. Ford, F. Jensen, A. Johnson, M. Krohn, E. MacDonald, T. Mulholland, R. Patel, A. Perloff, K. Stenson, K. A. Ulmer, S. R. Wagner

Cornell University, Ithaca, USA
J. Alexander, J. Chaves, Y. Cheng, J. Chu, A. Datta, K. Mcdermott, N. Mirman, J. R. Patterson, D. Quach, A. Rinkevicius, A. Ryd, L. Skinnari, L. Soffi, S. M. Tan, Z. Tao, J. Thom, J. Tucker, P. Wittich, M. Zientek

Fermi National Accelerator Laboratory, Batavia, USA
S. Abdullin, M. Albrow, M. Alyari, G. Apollinari, A. Apresyan, A. Apyan, S. Banerjee, L. A. T. Bauerdick, A. Beretvas, J. Berryhill, P. C. Bhat, K. Burkett, J. N. Butler, A. Canepa, G. B. Cerati, H. W. K. Cheung, F. Chlebana, M. Cremonesi, J. Duarte, V. D. Elvira, J. Freeman, Z. Gecse, E. Gottschalk, L. Gray, D. Green, S. Grünendahl, O. Gutsche, J. Hanlon, R. M. Harris, S. Hasegawa, J. Hirschauer, Z. Hu, B. Jayatilaka, S. Jindariani, M. Johnson, U. Joshi, B. Klima, M. J. Kortelainen, B. Kreis, S. Lammel, D. Lincoln, R. Lipton, M. Liu, T. Liu, J. Lykken, K. Maeshima, J. M. Marraffino, D. Mason, P. McBride, P. Merkel, S. Mrenna, S. Nahn, V. O'Dell, K. Pedro, C. Pena, O. Prokofyev, G. Rakness, L. Ristori, A. Savoy-Navarro[67], B. Schneider, E. Sexton-Kennedy, A. Soha, W. J. Spalding, L. Spiegel, S. Stoynev, J. Strait, N. Strobbe, L. Taylor, S. Tkaczyk, N. V. Tran, L. Uplegger, E. W. Vaandering, C. Vernieri, M. Verzocchi, R. Vidal, M. Wang, H. A. Weber, A. Whitbeck

University of Florida, Gainesville, USA
D. Acosta, P. Avery, P. Bortignon, D. Bourilkov, A. Brinkerhoff, L. Cadamuro, A. Carnes, D. Curry, R. D. Field, S. V. Gleyzer, B. M. Joshi, J. Konigsberg, A. Korytov, K. H. Lo, P. Ma, K. Matchev, H. Mei, G. Mitselmakher, D. Rosenzweig, K. Shi, D. Sperka, J. Wang, S. Wang, X. Zuo

Florida International University, Miami, USA
Y. R. Joshi, S. Linn

Florida State University, Tallahassee, USA
A. Ackert, T. Adams, A. Askew, S. Hagopian, V. Hagopian, K. F. Johnson, T. Kolberg, G. Martinez, T. Perry, H. Prosper, A. Saha, C. Schiber, R. Yohay

Florida Institute of Technology, Melbourne, USA
M. M. Baarmand, V. Bhopatkar, S. Colafranceschi, M. Hohlmann, D. Noonan, M. Rahmani, T. Roy, F. Yumiceva

University of Illinois at Chicago (UIC), Chicago, USA
M. R. Adams, L. Apanasevich, D. Berry, R. R. Betts, R. Cavanaugh, X. Chen, S. Dittmer, O. Evdokimov, C. E. Gerber, D. A. Hangal, D. J. Hofman, K. Jung, J. Kamin, C. Mills, I. D. Sandoval Gonzalez, M. B. Tonjes, H. Trauger, N. Varelas, H. Wang, X. Wang, Z. Wu, J. Zhang

The University of Iowa, Iowa City, USA
M. Alhusseini, B. Bilki[68], W. Clarida, K. Dilsiz[69], S. Durgut, R. P. Gandrajula, M. Haytmyradov, V. Khristenko, J.-P. Merlo, A. Mestvirishvili, A. Moeller, J. Nachtman, H. Ogul[70], Y. Onel, F. Ozok[71], A. Penzo, C. Snyder, E. Tiras, J. Wetzel

Johns Hopkins University, Baltimore, USA
B. Blumenfeld, A. Cocoros, N. Eminizer, D. Fehling, L. Feng, A. V. Gritsan, W. T. Hung, P. Maksimovic, J. Roskes, U. Sarica, M. Swartz, M. Xiao, C. You

The University of Kansas, Lawrence, USA
A. Al-bataineh, P. Baringer, A. Bean, S. Boren, J. Bowen, A. Bylinkin, J. Castle, S. Khalil, A. Kropivnitskaya, D. Majumder, W. Mcbrayer, M. Murray, C. Rogan, S. Sanders, E. Schmitz, J. D. Tapia Takaki, Q. Wang

Kansas State University, Manhattan, USA
S. Duric, A. Ivanov, K. Kaadze, D. Kim, Y. Maravin, D. R. Mendis, T. Mitchell, A. Modak, A. Mohammadi, L. K. Saini, N. Skhirtladze

Lawrence Livermore National Laboratory, Livermore, USA
F. Rebassoo, D. Wright

University of Maryland, College Park, USA
A. Baden, O. Baron, A. Belloni, S. C. Eno, Y. Feng, C. Ferraioli, N. J. Hadley, S. Jabeen, G. Y. Jeng, R. G. Kellogg, J. Kunkle, A. C. Mignerey, S. Nabili, F. Ricci-Tam, Y. H. Shin, A. Skuja, S. C. Tonwar, K. Wong

Massachusetts Institute of Technology, Cambridge, USA
D. Abercrombie, B. Allen, V. Azzolini, A. Baty, G. Bauer, R. Bi, S. Brandt, W. Busza, I. A. Cali, M. D'Alfonso, Z. Demiragli, G. Gomez Ceballos, M. Goncharov, P. Harris, D. Hsu, M. Hu, Y. Iiyama, G. M. Innocenti, M. Klute, D. Kovalskyi, Y.-J. Lee, P. D. Luckey, B. Maier, A. C. Marini, C. Mcginn, C. Mironov, S. Narayanan, X. Niu, C. Paus, C. Roland, G. Roland, G. S. F. Stephans, K. Sumorok, K. Tatar, D. Velicanu, J. Wang, T. W. Wang, B. Wyslouch, S. Zhaozhong

University of Minnesota, Minneapolis, USA
A. C. Benvenuti†, R. M. Chatterjee, A. Evans, P. Hansen, J. Hiltbrand, Sh. Jain, S. Kalafut, Y. Kubota, Z. Lesko, J. Mans, N. Ruckstuhl, R. Rusack, M. A. Wadud

University of Mississippi, Oxford, USA
J. G. Acosta, S. Oliveros

University of Nebraska-Lincoln, Lincoln, USA
E. Avdeeva, K. Bloom, D. R. Claes, C. Fangmeier, F. Golf, R. Gonzalez Suarez, R. Kamalieddin, I. Kravchenko, J. Monroy, J. E. Siado, G. R. Snow, B. Stieger

State University of New York at Buffalo, Buffalo, USA
A. Godshalk, C. Harrington, I. Iashvili, A. Kharchilava, C. Mclean, D. Nguyen, A. Parker, S. Rappoccio, B. Roozbahani

Northeastern University, Boston, USA
G. Alverson, E. Barberis, C. Freer, Y. Haddad, A. Hortiangtham, D. M. Morse, T. Orimoto, R. Teixeira De Lima, T. Wamorkar, B. Wang, A. Wisecarver, D. Wood

Northwestern University, Evanston, USA
S. Bhattacharya, J. Bueghly, O. Charaf, K. A. Hahn, N. Mucia, N. Odell, M. H. Schmitt, K. Sung, M. Trovato, M. Velasco

University of Notre Dame, Notre Dame, USA
R. Bucci, N. Dev, M. Hildreth, K. Hurtado Anampa, C. Jessop, D. J. Karmgard, N. Kellams, K. Lannon, W. Li, N. Loukas, N. Marinelli, F. Meng, C. Mueller, Y. Musienko[35], M. Planer, A. Reinsvold, R. Ruchti, P. Siddireddy, G. Smith, S. Taroni, M. Wayne, A. Wightman, M. Wolf, A. Woodard

The Ohio State University, Columbus, USA
J. Alimena, L. Antonelli, B. Bylsma, L. S. Durkin, S. Flowers, B. Francis, C. Hill, W. Ji, T. Y. Ling, W. Luo, B. L. Winer

Princeton University, Princeton, USA
S. Cooperstein, P. Elmer, J. Hardenbrook, S. Higginbotham, A. Kalogeropoulos, D. Lange, M. T. Lucchini, J. Luo, D. Marlow, K. Mei, I. Ojalvo, J. Olsen, C. Palmer, P. Piroué, J. Salfeld-Nebgen, D. Stickland, C. Tully

University of Puerto Rico, Mayaguez, USA
S. Malik, S. Norberg

Purdue University, West Lafayette, USA
A. Barker, V. E. Barnes, S. Das, L. Gutay, M. Jones, A. W. Jung, A. Khatiwada, B. Mahakud, D. H. Miller, N. Neumeister, C. C. Peng, S. Piperov, H. Qiu, J. F. Schulte, J. Sun, F. Wang, R. Xiao, W. Xie

Purdue University Northwest, Hammond, USA
T. Cheng, J. Dolen, N. Parashar

Rice University, Houston, USA
Z. Chen, K. M. Ecklund, S. Freed, F. J. M. Geurts, M. Kilpatrick, W. Li, B. P. Padley, J. Roberts, J. Rorie, W. Shi, Z. Tu, A. Zhang

University of Rochester, Rochester, USA
A. Bodek, P. de Barbaro, R. Demina, Y. t. Duh, J. L. Dulemba, C. Fallon, T. Ferbel, M. Galanti, A. Garcia-Bellido, J. Han, O. Hindrichs, A. Khukhunaishvili, E. Ranken, P. Tan, R. Taus

Rutgers, The State University of New Jersey, Piscataway, USA
A. Agapitos, J. P. Chou, Y. Gershtein, E. Halkiadakis, A. Hart, M. Heindl, E. Hughes, S. Kaplan, R. Kunnawalkam Elayavalli, S. Kyriacou, A. Lath, R. Montalvo, K. Nash, M. Osherson, H. Saka, S. Salur, S. Schnetzer, D. Sheffield, S. Somalwar, R. Stone, S. Thomas, P. Thomassen, M. Walker

University of Tennessee, Knoxville, USA
A. G. Delannoy, J. Heideman, G. Riley, S. Spanier

Texas A & M University, College Station, USA
O. Bouhali[72], A. Celik, M. Dalchenko, M. De Mattia, A. Delgado, S. Dildick, R. Eusebi, J. Gilmore, T. Huang, T. Kamon[73], S. Luo, R. Mueller, D. Overton, L. Perniè, D. Rathjens, A. Safonov

Texas Tech University, Lubbock, USA
N. Akchurin, J. Damgov, F. De Guio, P. R. Dudero, S. Kunori, K. Lamichhane, S. W. Lee, T. Mengke, S. Muthumuni, T. Peltola, S. Undleeb, I. Volobouev, Z. Wang

Vanderbilt University, Nashville, USA
S. Greene, A. Gurrola, R. Janjam, W. Johns, C. Maguire, A. Melo, H. Ni, K. Padeken, J. D. Ruiz Alvarez, P. Sheldon, S. Tuo, J. Velkovska, M. Verweij, Q. Xu

University of Virginia, Charlottesville, USA
M. W. Arenton, P. Barria, B. Cox, R. Hirosky, M. Joyce, A. Ledovskoy, H. Li, C. Neu, T. Sinthuprasith, Y. Wang, E. Wolfe, F. Xia

Wayne State University, Detroit, USA
R. Harr, P. E. Karchin, N. Poudyal, J. Sturdy, P. Thapa, S. Zaleski

University of Wisconsin-Madison, Madison, WI, USA
M. Brodski, J. Buchanan, C. Caillol, D. Carlsmith, S. Dasu, I. De Bruyn, L. Dodd, B. Gomber, M. Grothe, M. Herndon, A. Hervé, U. Hussain, P. Klabbers, A. Lanaro, K. Long, R. Loveless, T. Ruggles, A. Savin, V. Sharma, N. Smith, W. H. Smith, N. Woods

† **Deceased**

1: Also at Vienna University of Technology, Vienna, Austria
2: Also at IRFU, CEA, Université Paris-Saclay, Gif-sur-Yvette, France
3: Also at Universidade Estadual de Campinas, Campinas, Brazil
4: Also at Federal University of Rio Grande do Sul, Porto Alegre, Brazil
5: Also at Université Libre de Bruxelles, Bruxelles, Belgium
6: Also at University of Chinese Academy of Sciences, Beijing, China
7: Also at Institute for Theoretical and Experimental Physics, Moscow, Russia
8: Also at Joint Institute for Nuclear Research, Dubna, Russia
9: Also at Suez University, Suez, Egypt
10: Now at British University in Egypt, Cairo, Egypt
11: Also at Zewail City of Science and Technology, Zewail, Egypt
12: Also at Department of Physics, King Abdulaziz University, Jeddah, Saudi Arabia
13: Also at Université de Haute Alsace, Mulhouse, France
14: Also at Skobeltsyn Institute of Nuclear Physics, Lomonosov Moscow State University, Moscow, Russia
15: Also at CERN, European Organization for Nuclear Research, Geneva, Switzerland
16: Also at RWTH Aachen University, III. Physikalisches Institut A, Aachen, Germany
17: Also at University of Hamburg, Hamburg, Germany
18: Also at Brandenburg University of Technology, Cottbus, Germany
19: Also at MTA-ELTE Lendület CMS Particle and Nuclear Physics Group, Eötvös Loránd University, Budapest, Hungary
20: Also at Institute of Nuclear Research ATOMKI, Debrecen, Hungary
21: Also at Institute of Physics, University of Debrecen, Debrecen, Hungary
22: Also at Indian Institute of Technology Bhubaneswar, Bhubaneswar, India
23: Also at Institute of Physics, Bhubaneswar, India
24: Also at Shoolini University, Solan, India
25: Also at University of Visva-Bharati, Santiniketan, India
26: Also at Isfahan University of Technology, Isfahan, Iran
27: Also at Plasma Physics Research Center, Science and Research Branch, Islamic Azad University, Tehran, Iran
28: Also at Università degli Studi di Siena, Siena, Italy
29: Also at Scuola Normale e Sezione dell'INFN, Pisa, Italy
30: Also at Kyunghee University, Seoul, Korea
31: Also at International Islamic University of Malaysia, Kuala Lumpur, Malaysia
32: Also at Malaysian Nuclear Agency, MOSTI, Kajang, Malaysia
33: Also at Consejo Nacional de Ciencia y Tecnología, Mexico City, Mexico
34: Also at Warsaw University of Technology, Institute of Electronic Systems, Warsaw, Poland
35: Also at Institute for Nuclear Research, Moscow, Russia
36: Now at National Research Nuclear University 'Moscow Engineering Physics Institute' (MEPhI), Moscow, Russia
37: Also at St. Petersburg State Polytechnical University, St. Petersburg, Russia
38: Also at University of Florida, Gainesville, USA
39: Also at P.N. Lebedev Physical Institute, Moscow, Russia
40: Also at California Institute of Technology, Pasadena, USA
41: Also at Budker Institute of Nuclear Physics, Novosibirsk, Russia
42: Also at Faculty of Physics, University of Belgrade, Belgrade, Serbia
43: Also at INFN Sezione di Pavia[a], Università di Pavia[b], Pavia, Italy
44: Also at University of Belgrade, Faculty of Physics and Vinca Institute of Nuclear Sciences, Belgrade, Serbia
45: Also at National and Kapodistrian University of Athens, Athens, Greece
46: Also at Riga Technical University, Riga, Latvia
47: Also at Universität Zürich, Zurich, Switzerland

48: Also at Stefan Meyer Institute for Subatomic Physics (SMI), Vienna, Austria
49: Also at Adiyaman University, Adiyaman, Turkey
50: Also at Istanbul Aydin University, Istanbul, Turkey
51: Also at Mersin University, Mersin, Turkey
52: Also at Piri Reis University, Istanbul, Turkey
53: Also at Gaziosmanpasa University, Tokat, Turkey
54: Also at Ozyegin University, Istanbul, Turkey
55: Also at Izmir Institute of Technology, Izmir, Turkey
56: Also at Marmara University, Istanbul, Turkey
57: Also at Kafkas University, Kars, Turkey
58: Also at Istanbul University, Faculty of Science, Istanbul, Turkey
59: Also at Istanbul Bilgi University, Istanbul, Turkey
60: Also at Hacettepe University, Ankara, Turkey
61: Also at Rutherford Appleton Laboratory, Didcot, United Kingdom
62: Also at School of Physics and Astronomy, University of Southampton, Southampton, United Kingdom
63: Also at Monash University, Faculty of Science, Clayton, Australia
64: Also at Bethel University, St. Paul, USA
65: Also at Karamanoğlu Mehmetbey University, Karaman, Turkey
66: Also at Utah Valley University, Orem, USA
67: Also at Purdue University, West Lafayette, USA
68: Also at Beykent University, Istanbul, Turkey
69: Also at Bingol University, Bingol, Turkey
70: Also at Sinop University, Sinop, Turkey
71: Also at Mimar Sinan University, Istanbul, Istanbul, Turkey
72: Also at Texas A&M University at Qatar, Doha, Qatar
73: Also at Kyungpook National University, Daegu, Korea